Udmurt State University
Mathematical Institute SANU (Belgrade)
Steklov Mathematical Institute RAS (Moscow)
Journal "Regular and Chaotic Dynamics"
Russian Foundation of Basic Research

Sixth International Conference

"Geometry, Dynamics, Integrable Systems – GDIS 2016"

Book of Abstracts

2–5 June 2016

Izhevsk, Russia

The conference “Geometry, Dynamics, Integrable Systems – GDIS 2016” is being held under the auspices of the Russian Foundation for Basic Research (16-01-20252).

Sixth International Conference “Geometry, Dynamics, Integrable Systems – GDIS 2016”: Book of abstracts. — Moscow–Izhevsk: Publishing Center “Institute of Computer Science”, 2016. — 70 p.

ISBN 978-5-4344-0361-0

SCIENTIFIC COMMITTEE

Chair:

Alexey V. Borisov, Institute of Computer, Udmurt State University, Izhevsk, Russia

Valery Kozlov, V.A. Steklov Mathematical Institute of Russian Academy of Sciences, Russia

Vladimir Dragovic, Mathematical Institute SANU, Serbia

Alain Albouy, Institut de mécanique céleste et de calcul des éphémérides, ASD, France

Andrey Agrachev, V.A. Steklov Mathematical Institute of Russian Academy of Sciences, Russia

Alexey Bolsinov, School of Mathematics, Loughborough University, UK

Alexander Ivanov, Moscow Institute of Physics and Technology, Moscow, Russia

Sergey Kuznetsov, Kotel'nikov's Institute of Radio-Engineering and Electronics of RAS, Russia

Ivan Mamaev, Udmurt State University, Izhevsk, Russia

Dmitry Treschev, V.A. Steklov Mathematical Institute of Russian Academy of Sciences, Russia

Yuri Sachkov, Program Systems Institute of RAS, Russia

Oliver O'Reilly, University of California, USA

ORGANIZING COMMITTEE

Alexey Borisov, borisov@rcd.ru

Vladimir Dragovic, vladad@turing.mi.sanu.ac.rs

Nadezhda Erdakova, enn@rcd.ru

Alexander Kilin, aka@rcd.ru

Ivan Mamaev, mamaev@rcd.ru

Milena Radnovic, milena.radnovic@gmail.com

Switching in time-optimal problems

Andrey Agrachev

SISSA, Trieste, Italy & MIAN, Moscow, Russia

We study the time-optimal problem for generic control-affine system of the form:

$$\dot{x} = f_0(x) + \sum_{i=1}^{n} u_i f_i(x), \quad x \in \mathbb{R}^{n+1}, \quad \sum_{i=1}^{n} u_i^2 \leq 1,$$

and try to decode the structure of jump discontinuities of the optimal control in terms of Lie bracket relations between the vector fields $f_0, f_1, \ldots f_n$. Pontryagin Maximum Principle, the blow-up procedure, and elementary hyperbolic dynamics allow to reduce the problem to the study of an explicitly integrable dynamical system on the sphere S^{n-1}.

On a question by Wintner about the classification of the isosceles solutions of the 3-body problem

Alain Albouy[1], Hildeberto Cabral[2]

[1] *Observatoire de Paris, Paris, France*
[2] *Universidade Federal de Pernambuco, Recife, Brasil*

An isosceles solution of the Newtonian 3-body problem is a solution where the triangle formed by the 3 bodies remains isosceles all the time. In [2], Aurel Wintner recalls that *in any such solution either the 2 bodies at the base of the triangle have same mass, or the triangle is always equilateral*. He sketches in two pages a proof due to W. D. MacMillan and to J. Chazy and concludes, at page 315: "It would, of course, be desirable to find a proof based on dynamical, rather than on function-theoretical, principles. But it is quite doubtful that such proof exists. At any rate, the result is very deep, apparently much deeper than [the classification of the homographic solutions]."

We present a simpler proof which avoids complex analysis. We reduce the question to the examination of the conservation of energy on a candidate orbit which is obtained by a simple quadrature. The strange fact is that this candidate orbit could not be excluded by examining its qualitative behavior. It indeed visits the most interesting "allures finales" in Chazy's classification. For example, the candidate orbit can mimic a hyperbolic-parabolic escape at time $-\infty$ and a "continuable" hyperbolic escape at time $+\infty$. Chazy stated the conditions for the existence of an analytical continuation of an orbit of the n-body problem when the configuration reaches infinity in time and space. The candidate orbit does satisfy these conditions and indeed a continuation is proposed by the formula.

References

[1] Cabral, H. E. *On the isosceles solutions of the three-body problem*, 2012, Bol. Soc. Mat. Mexicana (3), 18, pp. 135–141

[2] Wintner A., *The Analytical Foundations of Celestial Mechanics.* Princeton Univ. Press, 1941

Nilpotent approximation of mobile robot with a trailer

Andrey Ardentov, Yu. Sachkov and A. Pichugin

[1] *Program Systems Institute of RAS, Pereslavl-Zalesskiy, Russia*

Different models of mobile wheel robot with a trailer can be defined by the following differential system:

$$
\begin{aligned}
\dot{x} &= u_1 \cos\theta, \\
\dot{y} &= u_1 \sin\theta, \\
\dot{\theta} &= u_2, \\
\dot{\varphi} &= -\frac{u_1}{l_t}\sin\varphi - \frac{l_r u_2}{l_t}\cos u_2 - u_2,
\end{aligned}
$$

where u_1, u_2 are controls which correspond to linear and angular velocity of the robot, coordinates (x, y, θ, φ) give the state of the mobile robot with a trailer on the plane. Constants $l_t > 0, l_r \geq 0$ set the model of connection of mobile robot and trailer [1].

The problem of translation mobile robot with a trailer from one state to another is difficult task even without cost functional. There are different approaches to solve this problem for some models, most of them developed for particular models and use their specifics. Our approach is based on concept of nilpotent approximation, which can be applied to every model of mobile robot with a trailer. This approach use solution of nilpotent sub-Riemannian problem on the Engel group, which is given by differential system

$$
\begin{aligned}
\dot{x} &= u_1, \\
\dot{y} &= u_2, \\
\dot{z} &= \frac{-u_1 y + u_2 x}{2}, \\
\dot{v} &= u_2 \frac{x^2 + y^2}{2}
\end{aligned}
$$

with the boundary conditions

$$
\begin{aligned}
&x(0) = y(0) = z(0) = v(0) = 0, \\
&x(t_1) = x_1, \quad y(t_1) = y_1, \quad z(t_1) = z_1, \quad v(t_1) = v_1
\end{aligned}
$$

and cost functional

$$\int_0^{t_1} \sqrt{u_1^2 + u_2^2}\, dt \to \min .$$

This optimal control problem was recently studied in works [2, 3, 4] and was reduced to solving a system of algebraic equations. Software for computation of optimal solutions will allow us to solve the motion planning problem for generic control systems with 4 states and 2 linear inputs via nilpotent approximation (in particular, for the kinematic model of mobile robot with a trailer).

The work is supported by the Russian Foundation for Basic Research (project no. 16-31-00396).

References

[1] Laumond J.-P., *Nonholonomic Motion Planning for Mobile Robots*. Tutorial notes, 1998, 112 p.

[2] Ardentov A. A., Sachkov Yu. L., *Extremal trajectories in nilpotent sub-Riemannian problem on the Engel group* // Sbornik: Mathematics, 2011, vol. 202, no. 11, pp. 1593–1615.

[3] Ardentov A. A., Sachkov Yu. L., *Conjugate points in nilpotent sub-Riemannian problem on the Engel group* // Journal of Mathematical Sciences, 2013, vol. 195, no. 3, pp. 369–390.

[4] Ardentov A. A., Sachkov Yu. L., *Cut time in sub-riemannian problem on engel group* // ESAIM: COCV, 2015, Vol. 21, no. 4, pp. 958–988.

Bifurcation and chaos exhibited by a rattleback lying on vibrating surface modified by magnetic force

Jan Awrejcewicz[1], Grzegorz Kudra[1]

[1]*Department of Automation, Biomechanics and Mechatronics, Lodz University of Technology, Lodz, Poland*

The present work concerns the problem of modelling, numerical simulations and analysis of bifurcation dynamics of a Celtic stone situated on a vibrating platform. The Celtic stone, also known as a wobblestone or a rattleback, usually is a semi-ellipsoidal rigid body lying on a flat and horizontal surface. The important property of the celt is non-coincidence of the principal axes of inertia and the principal directions of curvature at the equilibrium contact point. This leads to special dynamical properties of the wobblestone, i.e. if it is set in rotational motion around a vertical axis, it possess a "preferred" direction of spin. Dynamics of the celt under assumption of rolling without sliding was investigated in the work [1]. In the present work we investigate its properties in the case of harmonic motion of the platform. Similar investigations were performed and presented in the work [2], but only horizontal motion of the platform was taken into account. Here we assume linear (translational) vibrations in any direction. The contact forces are modelled in detail based on the work [3]. Moreover, a special additional force acting between the celt and the platform is assumed. It can be realized as a force between two permanent magnets. As the investigations showed, this force can modify the dynamic characteristics of the celt. It is important from the point of view of possible use of the rattleback as energy harvesting system [4].

The mechanical concept of the system is presented in Fig. 1. The semi-ellipsoidal body of geometry center at the point O and mass center at the point C with relative position described by vector $\mathbf{k}$, touches the plane and horizontal surface π at the point A. It is assumed that the platform moves translationally with acceleration $\mathbf{a}_b$. The governing equations reads

$$m\frac{d\mathbf{v}}{dt}+\boldsymbol{\omega}\times(m\mathbf{v})=-mg\mathbf{n}+\hat{N}\mathbf{n}+\hat{\mathbf{T}}_s+\mathbf{F}_m+\mathbf{F}_b,\quad \frac{d\mathbf{r}_C}{dt}=\mathbf{v},\quad \mathbf{B}\frac{\tilde{d}\boldsymbol{\omega}}{dt}+\boldsymbol{\omega}\times(\mathbf{B}\boldsymbol{\omega})=(\mathbf{r}-\mathbf{k})\times\left(\hat{N}\mathbf{n}+\hat{\mathbf{T}}_s\right)+\hat{\mathbf{M}}_s+\hat{\mathbf{M}}_r,$$

$$\frac{d\psi}{dt}=\frac{\omega_3\cos\varphi-\omega_1\sin\varphi}{\cos\theta},\ \frac{d\theta}{dt}=\omega_1\cos\varphi+\omega_3\sin\varphi,\ \frac{d\varphi}{dt}=\omega_2+\tan\theta(\omega_1\sin\varphi-\omega_3\cos\varphi),\ (\mathbf{r}_C+\mathbf{r}+\mathbf{k})\cdot\mathbf{n}=\mathbf{0}\quad (1)$$

where m denotes mass of the body, $\mathbf{B}$ – tensor of inertia at the mass center, $\mathbf{v}$ – local velocity of mass center in the reference frame $GX_1X_2X_3$ attached to the platform, $\boldsymbol{\omega}$ – absolute angular velocity of the body, $\mathbf{r}_C=\mathbf{r}_{GC}$ – vector defining the position of mass center C with respect to the origin G of the reference frame $GX_1X_2X_3$, $\hat{N}$ – magnitude of normal component of platform reaction, $\mathbf{n}$ – unit vector normal to the base, $\hat{\mathbf{T}}_s$ – resulting friction force acting at the point A, $\hat{\mathbf{M}}_s$ – friction moment, $\hat{\mathbf{M}}_r$ – rolling resistance moment, $\mathbf{F}_m$ – magnetic force, $\mathbf{F}_b=-\mathbf{a}_b m=-(q_{X1}\sin(\omega_{X1}t)\mathbf{e}_{X1}+q_{X2}\sin(\omega_{X2}t)\mathbf{e}_{X2}+q_{X3}\sin(\omega_{X3}t)\mathbf{e}_{X3})m$ – inertia force related to the base motion acting at the mass center C ($\mathbf{e}_{Xi}$ is unit vector of axis X_i), $\mathbf{r}$ – vector indicating the position of the contact point A. The notation $d\mathbf{u}/dt$ stands for the derivative with respect to time of a vector $\mathbf{u}$ in the coordinate system $GX_1X_2X_3$, while $\tilde{d}\mathbf{u}/dt$ denotes the corresponding derivative in the body-fixed reference frame $Cx_1x_2x_3$. The orientation of the body is defined by the following sequence of three rotations about the axes of the system $Cx_1x_2x_3$: x_3 (by an angle ψ), x_1 (by an angle θ) and x_2 (by an angle φ). The components of a vector $\mathbf{u}$ in the reference frame $Cx_1x_2x_3$ are denoted as u_i (i=1,2,3). The components of tensor of inertia $\mathbf{B}$ in the same co-ordinate system are denoted as $\boldsymbol{B}=[[B_1\ \ -B_{12}\ \ -B_{13}]\ \ [-B_{12}\ \ B_2\ \ -B_{23}]\ \ [-B_{13}\ \ -B_{23}\ \ B_3]]^T$. The set of equations (1) consists of differential and algebraic equations – the last vector expression describes the fact that the point A always lies in the surface π. The contact forces (friction force and moment, rolling resistance) are modelled by the use of special approximations suitable for fast and realistic numerical simulations [3]. It is assumed that some kind of pair of magnets is mounted inside the stone and inside the platform, in such a way that, using some kind of simplification, the pulling magnetic force acts between the points C and M and its magnitude can be approximated as $F_m = F_0 \exp(c_1 l_m + c_2 l_m^2)$, where l_m is distance between the points C and G, while F_0, c_1 i c_2 are the parameters. Based on the data concerning two ball magnets, one can assume $c_1 = -150\ \mathrm{m}^{-1}$ and $c_2 = 1500\ \mathrm{m}^{-2}$.

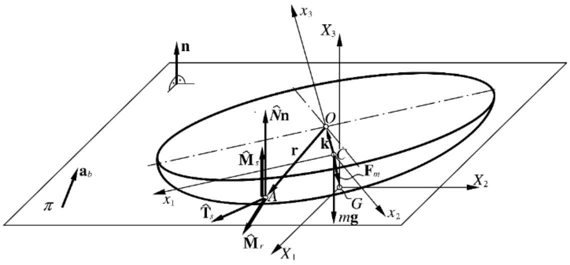

Fig. 1. The wobblestone.

In the presented below numerical examples the following parameters have been assumed: $m = 0.25\ \mathrm{kg}$, $g = 9.81\ \mathrm{m/s^2}$, $B_1 = 0.41 \cdot 10^3\ \mathrm{kg \cdot m^2}$, $B_2 = 2 \cdot 10^3\ \mathrm{kg \cdot m^2}$, $B_3 = 3.5 \cdot 10^3\ \mathrm{kg \cdot m^2}$, $B_{12} = -0.28 \cdot 10^3\ \mathrm{kg \cdot m^2}$, $B_{13} = B_{23} = 0$, $k_1 = k_2 = 0$, $k_3 = 0.006\ \mathrm{m}$, $a_1 = 0.08\ \mathrm{m}$, $a_2 = 0.016\ \mathrm{m}$, $a_3 = 0.012\ \mathrm{m}$ (semi-axes of the ellipsoid), $\mu = 0.2$ (friction coefficient), $\hat{a} = 0.001\ \mathrm{m}$ (radius of the contact), $f_r = 0.05\ \hat{a}$ (rolling resistance). The platform is assumed to vibrate only in normal direction - $q_{X1} = q_{X2} = 0$, $q_{X3} = 6\ \mathrm{m/s^2}$. In Fig. 2 there are presented bifurcation diagrams of the system with angular frequency ω_{X3} of vibrations playing a role of bifurcation parameter. One can also observe the influence of the magnetic force on the celt dynamics (F_0=0 in subfigure (a) and F_0=2 N in subfigure (b)), especially in the context of spin velocity ω_3 and potential use of the celt as energy harvesting system.

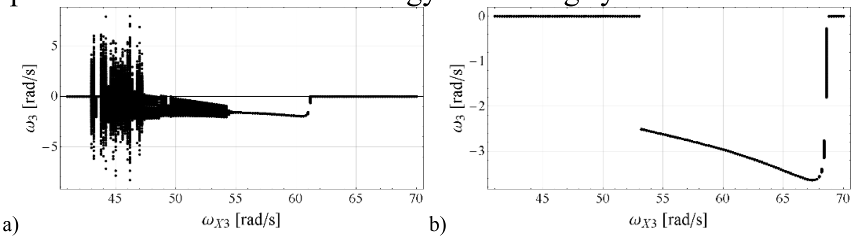

Fig. 2. Exemplary bifurcation diagrams – for F_0=0 (a) and F_0=2 N (b)

Acknowledgments. This work has been supported by the Polish National Science Centre, MAESTRO 2, No. 2012/04/A/ST8/00738.

References

[1] Borisov, A. V., Kilin, A.A., Mamaev, I.S. *New effects in dynamics of rattlebacks.* Doklady Physics, 2006, vol. 51, no. 5, pp. 272–275.

[2] Awrejcewicz, J., Kudra, G. *Mathematical modelling and simulation of the bifurcational wobblestone dynamics.* Discontinuity, Nonlinearity and Complexity, 2014, vol. 3, no. 2, pp. 123–132.

[3] Kudra, G., Awrejcewicz, J. *Application and experimental validation of new computational models of friction forces and rolling resistance.* Acta Mechanica, 2015, vol. 226, no. 9, pp. 2831–2848.

[4] Nanda, A., Singla, P., Karami, M. A. *Energy harvesting using rattleback: Theoretical analysis and simulations of spin resonance.* Journal of Sound and Vibration, 2016, vol. 369, pp. 195–208.

The special cases of degeneracy in the stability problem of an equilibrium position of a periodic Hamiltonian system

Boris S. Bardin

Department of Theoretical Mechanics,
Faculty of Applied Mathematics and Physics
Moscow Aviation Institute (National Research University)

We deal with the stability problem of an equilibrium position of a periodic Hamiltonian system with one degree of freedom. Hamiltonian is analytic in a small neighborhood of the equilibrium position and its normal form starts from terms of a certain order N ($N>2$). Usually, the stability character of the equilibrium depends only on nonzero terms of the lowest order N ($N>2$) in the Hamiltonian normal form. If the stability question cannot be solved by taking into account the terms of order N, then we say that case of degeneracy takes place. In such a situation it is necessary to consider terms of order higher than N to solve the stability problem.

We represent general theorems of stability and instability, which allow to solve stability problem for almost all cases of degeneracy. We show how to use the above theorems in order to obtain new stability criteria for some special cases of degeneracy. We also discuss a gap in the proof of Sokolskii theorem on stability.

The work is carried out at the cost of the grant of the Russian Scientific Foundation (project № 14-21-00068) at the Moscow Aviation Institute (National Research University).

The integrable case of M. Adler and P. van Moerbeke – thirty years later: spectral curve, first integrals and bifurcation diagram

Eketerina O. Biryucheva[1], Sergey V. Sokolov[2] and Pavel E. Ryabov[2,3]

[1] *Lomonosov Moscow State University, Moscow, Russia*
[2] *Institute for Machines Science RAS, Moscow, Russia*
[3] *Financial University under Government of the Russian Federation, Moscow, Russia*

In 2016 it is 30 years since M. Adler and P. van Moerbeke discovered the general case of integrability on the Lie algebra $so(4)$. An explicit form of the additional integral was presented in the original paper [1]. Later Reyman and Semenov-Tian-Shansky [2], with the help of a special algebra $\mathfrak{g}_2$, gave the Lax representation $\dot{L}(\lambda) = [L(\lambda), A(\lambda)]$. Other additional integrals different from that in [1] were presented by Bolsinov and Borisov [3] and V. Sokolov [4].

From the mechanical point of view the case of M. Adler and P. van Moerbeke can be reduced to the system governed by the Lamb-Poincare-Zhukovskii equations

$$\dot{\boldsymbol{M}} = \boldsymbol{M} \times \frac{\partial H}{\partial \boldsymbol{M}}, \quad \dot{\boldsymbol{S}} = \boldsymbol{S} \times \frac{\partial H}{\partial \boldsymbol{S}} \tag{1}$$

which describe the motion of a rigid body with an ellipsoidal cavity filled by a perfect incompressible vortical fluid around a fixed point. Here the 3-dimensional vector $\boldsymbol{M}$ denotes the angular momentum of the 'body+fluid' system and the components of $\boldsymbol{S}$ are proportional to the fluid's vorticity.

The Hamiltonian H is the kinetic energy of the 'body+fluid' system expressed in terms of $(\boldsymbol{M}, \boldsymbol{S})$

$$H = (\boldsymbol{M}, A\boldsymbol{M}) + 2(\boldsymbol{M}, B\boldsymbol{S}) + (\boldsymbol{S}, C\boldsymbol{S}).$$

Here A, B and C are diagonal 3×3 matrices which read

$$\begin{aligned}
&A = \operatorname{diag}\left[\alpha_2^2\alpha_3^2, \alpha_1^2\alpha_3^2, \alpha_1^2\alpha_2^2\right];\\
&B = \operatorname{diag}\left[(\alpha_1-\alpha_2)(\alpha_3-\alpha_1)\alpha_2\alpha_3, (\alpha_2-\alpha_1)(\alpha_3-\alpha_2)\alpha_1\alpha_3, (\alpha_3-\alpha_1)(\alpha_2-\alpha_3)\alpha_1\alpha_2\right];\\
&C = \operatorname{diag}\left[\alpha_2\alpha_3(\alpha_2\alpha_3-4\alpha_1^2), \alpha_1\alpha_3(\alpha_1\alpha_3-4\alpha_2^2), \alpha_1\alpha_2(\alpha_1\alpha_2-4\alpha_3^2)\right].
\end{aligned}$$

Besides the energy integral H, the equations (1) always have the geometric integrals

$$F_1 = (\boldsymbol{M}, \boldsymbol{M}), \qquad F_2 = (\boldsymbol{S}, \boldsymbol{S}),$$

which are the Casimir functions with respect to the Lie-Poisson bracket

$$\{M_i, M_j\} = \varepsilon_{ijk} M_k, \quad \{M_i, S_j\} = 0, \quad \{S_i, S_j\} = \frac{1}{3}\varepsilon_{ijk} S_k.$$

On the common level

$$\mathcal{P}_{a,b} = \{F_1 = a^2,\ F_2 = b^2\} \cong S^2 \times S^2$$

the induced Lie-Poisson bracket is non-degenerate and the system (1) restricted to this level gives an integrable Hamiltonian system with two degrees of freedom and with an additional integral K of the form

$$\begin{aligned}
K = 3\sum_{i,j} \alpha_i(\alpha_j-\alpha_i) M_j S_j S_i^2 + \sum_i (\alpha_i-\alpha_j)(\alpha_i-\alpha_k) M_i S_i^3 -\\
-(\boldsymbol{M}, \boldsymbol{M}) \sum_i \left[\alpha_j\alpha_k M_i S_i + 2(\alpha_j^2+\alpha_k^2) S_i^2\right].
\end{aligned}$$

If $\alpha_1 + \alpha_2 + \alpha_3 = 0$, then the integral K is in involution with Hamiltonian H.

It is well known that the invariants of the matrix $\mathrm{Tr}L(\lambda)^k$ are first integrals. This integrals generate a momentum map $\mathcal{F}$. At present we do not have a general theorem that links the structure of the bifurcation diagram (the image of the critical points of the momentum map) to the discriminant set of the algebraic curve $\Gamma(\lambda, \mu) = \det(L(\lambda) - \mu I)$. However as we can see from the study of specific mechanical systems [5], [6] such a link exists and it can be used as a hypothesis for the derivation of the equations of bifurcation diagram (with a subsequent proof of sufficiency).

Here, for the M. Adler and P. van Moerbeke case, we explicitly present the spectral curve $\Gamma(\lambda, \mu)$. This enables us upon the inspection of the curves singularities to find the bifurcation diagram of the momentum map $\mathcal{F}$. Here we also discuss the phase topology of that Hamiltonian system. In particular we find the bifurcation diagram of the momentum map and explore bifurcations of the Liouville tori. An example of the bifurcation diagram is presented in Fig. 1.

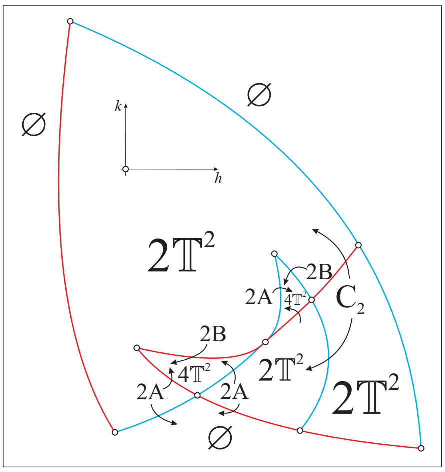

Fig. 1. Bifurcation diagram

This work is supported by the grants of RFBR Nos. 14-01-00119, 16-01-00170 and 16-01-00809 and also by grant of RFBR and Volgograd Region Authorities No 15-41-02049.

References

[1] Adler M., van Moerbeke P. *A new geodesic flow on* $so(4)$ // Prob., stat. mech. and numb. theory. Adv. in math. suppl. studies, 1986, vol. 9, pp. 81–96.

[2] Reyman A. G. and Semenov-Tian-Shansky M. A. *A New Integrable Case of the Motion of the 4-Dimensional Rigid Body* // Commun. Math. Phys., 1986, vol. 105, no. 3, pp. 461–472.

[3] Bolsinov A. V., Borisov A. V. *Compatible Poisson Brackets on Lie Algebras* // Math. Notes, 2002, vol. 72, no. 1, pp. 10–30.

[4] Borisov A. V., Mamaev I. S. *Rigid body dynamics. Hamiltonian methods, integrability, chaos* MoscowIzhevsk: Institute of Computer Science, 2005, p. 576.

[5] Ryabov P. E. *Phase topology of one irreducible integrable problem in the dynamics of a rigid body* // Theoret. and Math. Phys., 2013, vol. 176, no. 2, pp. 1000–1015.

[6] Ryabov P. E. *New invariant relations for the generalized two-field gyrostat* // Journal of Geometry and Physics, 2015, vol. 87, pp. 415–421.

The dynamics of vortex sources in a deformation flow

Ivan A. Bizyaev, Alexey V. Borisov and Ivan S. Mamaev

Institute of Computer Science, Udmurt State University, Izhevsk, Russia

In the classical hydrodynamics, the problem of the interaction of n point vortices in an ideal fluid on a plane and a sphere is well understood. Its distinctive feature is that the equations of motion of point vortices are represented in Hamiltonian form. Along with the above-mentioned model of point vortices, hydrodynamics uses other, more general, vortex models. Historically, the very first model was that of A. A. Fridman and P.Ya.Polubarinova [1] featuring the interaction of more complex point singularities combining vortex properties and the properties of sources and sinks, namely, the model of vortex sources. This paper is concerned with the dynamics of vortex sources in a deformation flow.

The equations of motion of n vortex sources in a deformation flow have the form

$$\begin{aligned} \dot{x}_i &= -\frac{1}{2\pi}\sum_{j\neq i}^{n}\frac{\Gamma_j(y_i-y_j)-\mathrm{K}_j(x_i-x_j)}{(x_i-x_j)^2+(y_i-y_j)^2}+by_i, \\ \dot{y}_i &= \frac{1}{2\pi}\sum_{j\neq i}^{n}\frac{\Gamma_j(x_i-x_j)+\mathrm{K}_j(y_i-y_j)}{(x_i-x_j)^2+(y_i-y_j)^2}-ax_i, \end{aligned} \tag{1}$$

where $i=1,..,n$.

The system (1) preserves the standard invariant measure:

$$\mu=\prod_{i=1}^{n}dx_i dy_i.$$

However, in the general case it is not Hamiltonian. Let us define the vector fields $\boldsymbol{u}_x$ and $\boldsymbol{u}_y$, corresponding to the shifts along the axes Ox and Oy

$$\boldsymbol{u}_x=\sum_{i=1}^{n}\frac{\partial}{\partial x_i},\quad \boldsymbol{u}_y=\sum_{i=1}^{n}\frac{\partial}{\partial y_i}, \tag{2}$$

and denote the vector field of the system (1) by $\boldsymbol{u}$. These vector fields form a solvable Lie algebra with respect to commutation operations:

$$[\boldsymbol{u}_x,\boldsymbol{u}]=-a\boldsymbol{u}_y,\quad [\boldsymbol{u}_y,\boldsymbol{u}]=b\boldsymbol{u}_x,\quad [\boldsymbol{u}_x,\boldsymbol{u}_y]=0. \tag{3}$$

Hence, according to the Lie theorem, one can reduce the order of the system (1) by two by choosing the integrals (2) as new variables.

The case of two vortex sources is shown to be integrable by quadratures. In addition, the relative equilibria (of the reduced system) are examined in detail and it is shown that in this case the trajectory of vortex sources is an ellipse.

References

[1] Fridman, A. A. and Polubarinova, P.Ya., On Moving Singularities of a Flat Motion of an Incompressible Fluid, Geofiz. Sb., 1928, vol. 5, no. 2, pp. 9–23 (Russian).

Degenerate billiards

Sergey Bolotin

Moscow Steklov Mathematical Institute, Russia
University of Wisconsin, USA

In an ordinary billiard trajectories of a Hamiltonian system are elastically reflected when colliding with a hypersurface (scatterer). If the scatterer is a submanifold of codimension more than one, then collisions are rare. Trajectories with infinite number of collisions form a lower dimensional dynamical system. Degenerate billiards appear as limits of ordinary billiards and and as limits of systems of light bodies in celestial mechanics.

Stability analysis, singularities and topology of integrable systems

Alexey Bolsinov

Loughborough University, UK

In the theory of integrable systems, there are two popular topics:

1) Topology of integrable systems, which studies stability of equilibria and periodic trajectories, bifurcations of Liouville tori, singularities and their invari- ants, topological obstructions to the integrability and so on.

2) Theory of compatible Poisson brackets, which studies one of the most in- teresting mechanisms for integrability based on the existence of a bi-Hamiltonian representation.

The aim of the talk is to to construct a bridge between these two areas and to explain how singularities of bi-Hamiltonian systems are related to algebraic properties of compatible Poisson brackets. This bridge provides new stability analysis methods for a wide class of integrable systems.

The Kovalevskaya top and its generalizations

Alexey Borisov, Ivan Mamaev

Udmurt State University, Izhevsk, Russia

We consider two issues concerning the idea of generalizing the classical system discovered by Kovalevskaya in rigid body dynamics.

One of the generalizations implies the possibility of introducing various additive terms which preserve the integrability of the classical Kovalevskaya case. This issue is considered in relation to the possibility of using quaternions in the description of rigid body dynamics and various more general problems involving the Kovalevskaya case (the Semenov–Tian-Shansky system and additive terms introduced by Sokolov and Yehia). The origin of these additive terms is explained.

The second generalization of the Kovalevskaya case is related to the development of Zhukovsky's idea of describing rigid body dynamics in the space of constant negative curvature, that is, in the Lobachevsky space. A form of the Euler–Poisson equations in these spaces is obtained and analogs of the classical integrable systems for this case are presented. In a particular case, a noncompact version of the Kovalevskaya case is considered and its differences from the classical case are discussed.

Electromagnetic waves in conformal actions of the group *SU*(2, 2) on a dimensional flat model of the space-time

Francisco Bulnes

Department in Mathematics and Engineering, TESCHA , Chalco, Mexico

The ultra-hyperbolic wave equation is satisfied using the Penrose integral over $P^3(\mathbb{C})$. But,considering the Lie group $SU(2,2)$, we can consider conformal theories of gauge fields as electromagnetic fields to measure other fields as gravity [1]. In both directions of a light cone appear the auto-dual Maxwell fields of positive frequency and negative frequency on *M* (the space-time) respectively that go being added in each time to each orbit. This corresponds to partial waves expansions in 2-dimensions considering the causal structure of the space-time given by these light cones in a 2-dimensional flat model of the space-time [2].

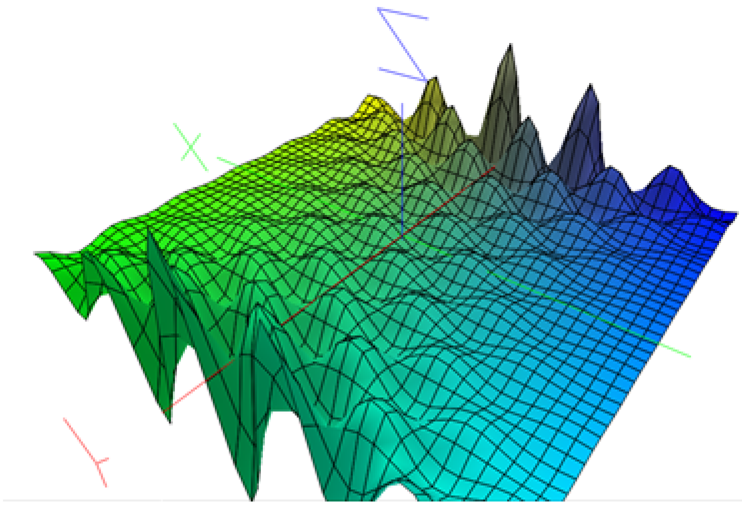

Fig. 1. Electromagnetic waves in conformal actions of the group $SU(2,2)$, on a $2-$dimensional flat model of the space-time. The ultra-hyperbolic wave equation is satisfied. In both sides of axis *Y*, appear the auto-dual Maxwell fields of positive frequency and negative frequency on *M*, respectively that go being added in each time to each orbit. This corresponds to partial waves expansions in 2-dimensions.

References

[1] Bulnes F. *Electromagnetic Gauges and Maxwell Lagrangians Applied to the Determination of Curvature in the Space-Time and their Applications*// Journal of Electromagnetic Analysis and Applications, 2012, vol. 4, no. 6, pp. 252–266. DOI: 10.4236/jemaa.2012.46035

[2] Bulnes F. *Mathematical Electrodynamics: Groups, Cohomology Classes, Unitary Representations, Orbits and Integral Transforms in Electro-Physics*// American Journal of Electromagnetics and Applications, 2015, vol. 3, no. 6, pp. 43-52 10.11648/j.ajea.20150306.12

Planar homogeneous potentials and Lotka Voltera systems

Thierry Combot

University of Burgundy, Dijon, France

Given an integrable rational planar potential, we can build a family of integrable potentials through rotation and dilatation. Taking singular limits, we can build limit potentials which are also integrable. These potentials have a special new homogeneity property: the potential gets multiplied after a rotation. We can build an analogue of Darboux points and integrability conditions similar to the Morales Ramis table. Some of these are bihomogeneous, and after a variable change are planar quadratic vector fields, Lotka Volterra systems. Thanks to M.Ollagnier classification of such integrable vector fields, this allows to build new integrability conditions for homogeneous potentials. There exists a relation between the eigenvalues of Hessian at Darboux points, however this relation does not always hold. We will prove that this relation in fact always hold except in few cases which are already known to be integrable. This opens the possibility to classify all integrable homogeneous polynomial potentials. Joint work with A.Maciejewski.

Four-dimensional generalization of the Grioli precession

Vladimir Dragović[1,2] and Borislav Gajić [1]

[1] *Mathematical Institute SANU, Belgrade, Serbia*
[2] *The Department of Mathematical Sciences, The University of Texas at Dallas, USA*

A particular solution of the four-dimensional Lagrange top on $e(4)$ representing a four-dimensional regular precession is constructed. Using it, a four-dimensional analogue of the Grioli nonvertical regular precession of an asymmetric heavy rigid body is constructed.

Twisting somersault and geometric phase

Holger Dullin

University of Sydney, School of Mathematics and Statistics, Sydney, Australia

The free flight of a springboard diver can be modelled by a non-rigid body, or a system of coupled rigid bodies. Given the shape change of the body we show that an Euler equation modified by a vector potential describes the dynamics. We derive the geometric phase for this model, and thus obtain a complete understanding of the twisting somersault. The simplest possible model is a a ``diver with a rotor''. This is a rigid body with a rotor attached, and the rotor can be switched on at off to control the dynamics. For more realistic models of human divers we propose a new dive with more twists then have ever been performed in competition.

On the dynamics of a tripod sliding on a smooth surface

Nadezhda Erdakova, Ivan Mamaev

Udmurt State University, Izhevsk, Russia

We investigate the dynamics of a body with three point supports (tripod) sliding on a horizontal rough plane. We assume that the body with mass m is dynamically consistent. This means that one of the principal axes of inertia coincides with the normal to the plane. The center of mass lies at height h on this axis. The positions of the supports of the body are determined by three radius vectors $\boldsymbol{r}_i = (x_i, y_i, -h)$, $i = 1, 2, 3$, respectively.

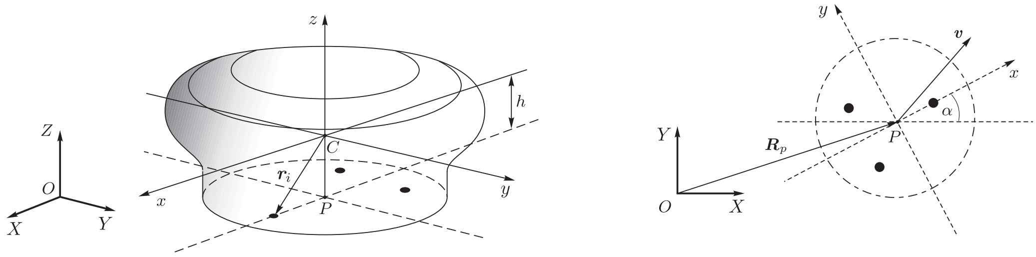

Figure 1. Rigid body with three point supports (tripod) sliding on a plane. $OXYZ$ is a fixed coordinate system and $Cxyz$ is a moving coordinate system with origin at the center of the mass.

We assume that the tripod slides under the action of the dry friction law of Amonton-Coulomb. In this case the equations of motion of this body in the fixed coordinate system $OXYZ$ can be represented as

$$\dot{X} = v_x \cos\alpha + v_y \sin\alpha, \quad \dot{Y} = -v_x \sin\alpha + v_y \cos\alpha, \quad \dot{\alpha} = \omega,$$

where X and Y are the coordinates of the center of mass, α is the angle of rotation of the moving coordinate system $Cxyz$ about the fixed coordinate system, v_x, v_y are the linear velocity components referred to the axes of $Cxyz$, and ω is the angular velocity. The velocities can be determined from the equations

$$m(\dot{v}_x - \omega v_y) = -f\sum_{i=1}^{3} N_i V_{xi}, \quad m(\dot{v}_y + \omega v_x) = -f\sum_{i=1}^{3} N_i V_{yi}, I_z\dot{\omega} = -f\sum_{i=1}^{3} N_i(x_i V_{yi} - y_i V_{xi}),$$

N_i are the normal reactions at contact points

$$N_1 = mg\frac{(a_2b_3 - b_2a_3)}{b_1(a_2 - a_3) + b_2(a_3 - a_1) + b_3(a_1 - a_2)}, N_2 = mg\frac{(a_3b_1 - b_3a_1)}{b_1(a_2 - a_3) + b_2(a_3 - a_1) + b_3(a_1 - a_2)},$$

$$N_3 = mg\frac{(a_1b_2 - b_1a_2)}{b_1(a_2 - a_3) + b_2(a_3 - a_1) + b_3(a_1 - a_2)}, a_i = x_i - fhV_{ix}, \ b_i = y_i - fhV_{iy},$$

$$V_{ix} = \frac{v_x - \omega y_i}{\sqrt{(v_x - \omega y_i)^2 + (v_y + \omega x_i)^2}}, V_{iy} = \frac{v_y + \omega x_i}{\sqrt{(v_x - \omega y_i)^2 + (v_y + \omega x_i)^2}},$$

g is the acceleration of gravity, f is the coefficient of friction, and I_z is the moment of inertia relative to the axis OZ.

To investigate the terminal motion of this system, we use the method of reduction presented in [1]. We find conditions for the existence of a stable translational motion depending on the positions of the supports of the body relative to the radius of inertia of the body. Also, it is shown that the terminal motion of the tripod can be pure rotation, pure sliding, or rotation and sliding cease simultaneously at the instant of stop.

We obtain trajectories in absolute space for different types of terminal motion and compare the results with the trajectories obtained in [2] for particular cases of rapid and slow rotation of the tripod.

References

[1] Treschev D.V., Erdakova N.N., Ivanova T.B. On the final motion of cylindrical solids on a rough plane // Rus. J. Nonlin. Dyn., 2012, vol. 8, no. 3, pp. 585–603 (Russian)

[2] Shegelski M.R.A., Goodvin G.L., Booth R., Bagnall P., Reid M. Exact normal forces and trajectories for a rotating tripod sliding on a smooth surface // Canadian J. Phys., 2004, vol. 82, pp. 875-890

A shortcut to the Kovalevskaya curves

Yuri N. Fedorov

Department of Mathematics, Polytechnic university of Catalonia, Barcelona, Spain

There have already been numerous studies and interpretations of the famous separation of variables in the integrable top of S. Kovalevskaya.

In this talk we generate the curves of separation of variables for this classical system and its integrable generalizations. In particular, we will show how the original Kovalevskaya curve of separation can be obtained, by a simple one-step transformation, from the spectral curve of the corresponding Lax representation found in [2]. The algorithm works for the general constants of motion of the top and is based on W. Barth's description of Prym varieties via pencils of genus 3 curves [1], which was given a further extension in [4, 3]. It also allows us to derive existing and new curves of separation for the Kovalevskaya gyrostat in one and two force fields.

References

[1] Barth, W. Abelian surfaces with $(1, 2)$-polarization. *Algebraic geometry, Sendai*, 1985, 41–84, Adv. Stud. Pure Math., **10**, North-Holland, Amsterdam, 1987.

[2] Bobenko A.I., Reyman A.G., and Semenov–Tian-Shansky M. *The Kowalewski top 99 year later: a Lax pair, generalizations and explicit solutions*, Commun. Math. Phys. **122**, (1989) 321–354

[3] Enolski V. Z., Fedorov, Yu. N. Algebraic description of Jacobians isogeneous to certain Prym varieties with polarization (1,2). arXiv:1411.6143v1 [nlin.SI] (2015)

[4] Horozov E., van Moerbeke P. The full geometry of Kowalewski's top and $(1, 2)$-abelian surfaces. *Comm. Pure Appl. Math.* **42**:4 (1989) 357–407

Modified LR and L+R systems and rolling spheres

Bozidar Jovanovic

Mathematical institute SANU, Serbia

We introduce a class of dynamical systems having an invariant measure, the modifications of well known systems on Lie groups: LR and L+R systems. As an example, we study modified Veselova nonholonomic rigid body problem, considered as a dynamical system on the product of the Lie algebra $so(n)$ with the Stiefel variety $V_{n,r}$, as well as the associated ϵL+R system on $so(n) \times V_{n,r}$. In the 3–dimensional case, these systems model the nonholonomic problems of a motion of a ball and a rubber ball over a fixed sphere.

On the control of the displacement of M-block

Alexander P. Ivanov

Moscow Institute of Physics and Technology,
Dolgoprudny, Moscow District, Russia

Momentum driven blocks (M-blocks) were created in the MIT in the context of solving the problem of constructing certain engineering devices during emergencies. The lattices of such blocks could be useful for repair bridges or buildings, or raise and reconfigure scaffolding for building projects [1]. Such system belongs to the family of mobile devices without external actuators: wheels, tracks, etc. A general advantage of these devices is their ability to work in off-road conditions as well as in the presence of high temperature or pressure. The M-block consists of cubic case and a flywheel, equipped with a motor and braking system (Fig. 1). The system is initially at rest on a flat surface. At a moment, the motor accelerates the flywheel without moving the case. Then the brakes kill the rotation, and in accordance with laws of dynamics, the angular momentum of the rotor is transferred to the case. Owing to friction forces, the block shifts in a new position or jumps on another block. This trick can be repeated until desirable configuration will be achieved. If the axle is parallel to an edge, then the system moves in the orthogonal plane [2]. In this paper we suggest that the rotor is inclined to the horizon. It is shown that in this case the block rotates around vertical, and when it falls to the ground, its orientation will change. Varying the inclination angle, one can transfer the block to any prescribed place.

The equations of impulsive motions of M-block were derived in [2], and their basic properties were established. The simplest case where the axle of flywheel is parallel to an edge of the cube was studied in detail owing the possibility of reduction to 2D formulation. In general case analytical solution seems impossible.

Fig. 1 The M-Block with its innards exposed and its flywheel

References

[1] Romanishin J. W., Gilpin K., Rus D., *M-blocks*: *Momentum-driven, magnetic modular Robots* // Intelligent Robots and Systems (IROS), IEEE/RSJ International Conference on, 2013, pp. 4288–4295.

[2] Ivanov A.P., *On impulsive dynamics of M-blocks* // Regular and Chaotic Dynamics, 2014, Vol. 19, No. 2, pp. 214–225.

Retrograde turn of rolling disk

Yuri L. Karavaev[1], Alexander A. Kilin[2]

[1] *Kalashnikov Izhevsk State Technical University, Izhevsk, Russia*
[2] *Udmurt State University, Izhevsk, Russia*

The dynamics of rolling disk is sufficiently well understood, but some questions remain regarding, for example, the loss of contact of the disk with the surface before it stops [2] or terminal retrograde turn of rolling disk with a central hole [1]. In the last paper M. A. Jalali et al. [1] explained the retrograde turn of rings by aerodynamic phenomena due to the presence of a central hole as opposed to a homogeneous disk. We conducted experiments that show air drag is not a reason for the retrograde turn of the ring during its rolling. A review of articles in this area has shown that there is turning effect of the rolling disk and spinning top. In our work we explain the phenomenon of the retrograde turn of the ring qualitatively within the framework of the model of a rolling ring with viscous rolling friction. This model is obtained by modification of nonholonomic model [3] taking into account rolling friction.

References

[1] Jalali, Mir Abbas and Sarebangholi, Milad S. and Alam, Mohammad-Reza, Terminal retrograde turn of rolling rings, Phys. Rev. E, 92, 032913, 2015, doi: 10.1103/ PhysRevE.92.032913.

[2] Borisov, A.V., Mamaev, I. S., and Karavaev, Yu. L., On the Loss of Contact of the Euler Disk, Nonlinear Dynam., 2015, vol. 79, no. 4, pp. 22872294.

[3] Borisov, A. V., Mamaev I. S., Kilin A. A., Dynamics of rolling disk, Regular and Chaotic Dynamics, 2003, vol. 8, no. 2, pp. 201-212.

Smale-Williams attractor in a modified Neimark model

Leila Khadzhieva[1] and Vyacheslav Kruglov[1,2]

[1] *Saratov State University, Saratov, Russia*
[2] *Radioengineering and Electronics Institute of RAS, Saratov Branch, Saratov, Russia*

Last years a number of systems with uniformly hyperbolic attractors were introduced [1, 2], mostly with Smale-Williams solenoid [1, 2]. The operation of these systems is based on a manipulation with angular variables [1, 2] (e.g. phases of oscillations). The angular variable should undergo Bernoulli map on each average time interval intrinsic to a system to make Smale-Williams attractor appear. There are some examples of autonomous systems with hyperbolic attractors [3]. The one in [3] is a minimal four-dimensional system similar to the predator-pray model composed of two oscillators possessing an attractor of the SmaleWilliams type. The other three examples in [3] are systems of three coupled oscillators with a heteroclinic cycle. There is also an example of distributed autonomous system with Smale-Williams attractor in [4].

We introduce an example of autonomous system with Smale-Williams solenoid as an attractor. The basic idea of its operation follows [3]. The model is composed of two subsystems that are Neimark systems with "figure-eight" ("double loop") homoclinics. We consider the coordinates of subsystems as real and imaginary parts of some complex variable. Due to coupling the argument of that variable undergoes Bernoulli map each time the trajectory comes close to a saddle.

The equations are:

$$\begin{aligned}
&\dot{x} = u,\\
&\dot{u} = (1 - x^2 - y^2)x + \left[L - (x^2 + y^2 - 1)^2\right] u + \varepsilon(u^3 + 3uv^2),\\
&\dot{y} = v,\\
&\dot{v} = (1 - x^2 - y^2)y + \left[L - (x^2 + y^2 - 1)^2\right] v + \varepsilon(3u^2 v - v^3),
\end{aligned} \tag{1}$$

where ε is coupling parameter. We rewrite them in complex form:

$$\begin{aligned}
&\dot{z} = w,\\
&\dot{w} = (1 - |z|^2)z + \left[L - (1 - |z|^2)^2\right] w + \varepsilon w^3,
\end{aligned} \tag{2}$$

where $z = x + iy$ and $w = u + iv$.

Lets explain the principle of its operation. The argument of z is an angular variable θ: $z = C\exp(i\theta)$. When absolute value of z is close to zero (the trajectory is close to a saddle point in the origin of coordinates) the angular variable triples due to the term εw^3 and cubic nonlinearity in $(1 - |z|^2)z$. Thus, the angular variable θ undergoes transformation according to the Bernoulli map $\theta_{n+1} = 3\theta_n + \mathrm{const}(\mathrm{mod}\ 2\pi)$ at each round required for the trajectory to get close to a saddle.

The equations (1) were solved numerically. Fig.1 demonstrates a portrait of attractor of system (1) ($L = 0.32$, $\varepsilon = 0.02$). Fig.2a shows a portrait of attractor in the Poincaré cross-section ($L = 0.32$, $\varepsilon = 0.02$). The cross-section surface is $S = x^2 + y^2 = 1$ (in direction of increase of S). Fig.2b demonstrates an iteration diagram for the angular variable (taken on every successful cross-section). It is close to iteration diagram of Bernoulli map: while angular variable θ passes from 0 to 2π, its image passes this interval three times.

Lyapunov exponents of the attractor in Poincaré cross-section were estimated by Benettin algorithm. The full spectrum of Lyapunov exponents for the Poincaré map is

$$\lambda_1 = 1.041, \quad \lambda_2 = -3.859, \quad \lambda_3 = -5.023.$$

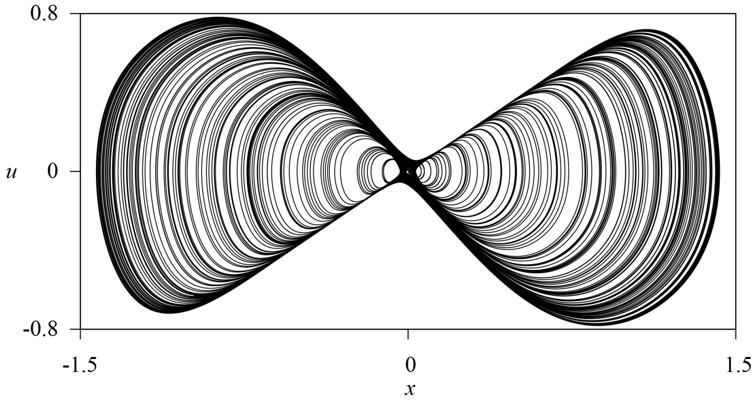

Fig. 1. A portrait of attractor of system (1) ($L = 0.32$, $\varepsilon = 0.02$).

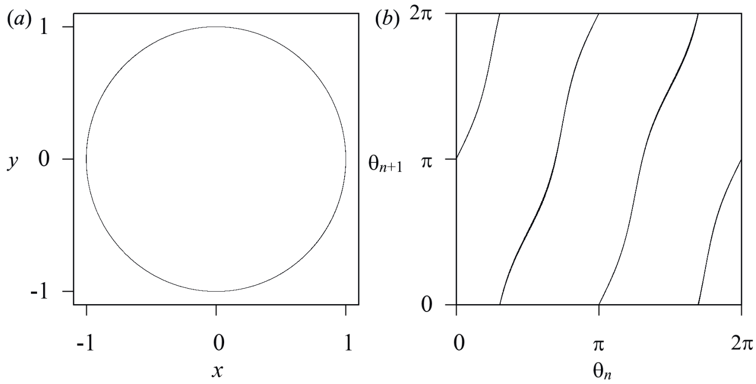

Fig. 2. (a) A portrait of attractor in Poincaré cross-section ($L = 0.32$, $\varepsilon = 0.02$); (b) an iteration diagram for angular variable θ (taken on every successful cross-section).

The largest Lyapunov exponent is close to $\log 3$ which is Lyapunov exponent for Bernoulli map. The rest exponents are negative. That corresponds to attractor of Smale-Williams type embedded in the three-dimensional state space of the Poincaré map.

The work was supported by RFBR grant No 16-32-00449.

References

[1] Kuznetsov S. P. *Hyperbolic Chaos: A Physicist's View.* Higher Education Press, Beijing and Springer-Verlag GmbH Berlin Heidelberg, 2012.

[2] Kuznetsov S. P. *Dynamical chaos and uniformly hyperbolic attractors: from mathematics to physics* // Physics-Uspekhi, 2011, vol. 54, no. 2, pp. 119144.

[3] Kuznetsov S. P., Pikovsky A. *Autonomous coupled oscillators with hyperbolic strange attractors* // Physica D: Nonlinear Phenomena, 2007, vol. 232, no. 2, pp. 87-102.

[4] Kruglov, V. P., Kuznetsov S. P., Pikovsky A. *Attractor of Smale-Williams type in an autonomous distributed system* // Regular and Chaotic Dynamics, 2014, vol. 19, no. 4, pp. 483-494.

Controllable two-dimensional motion of a rigid body in an ideal fluid

Evgenii V. Vetchanin[1,2], Alexander A. Kilin[2]

[1] *Kalashnikov Izhevsk State Technical University, Izhevsk, Russia*
[2] *Udmurt State University, Izhevsk, Russia*

In this paper we consider the controlled plane motion of a hydrodynamically asymmetric rigid body in an ideal fluid (see Fig. 1) for a constant magnitude of circulation Γ around the body. The body has mass M and central moment of inertia I, carries two material points with masses m_1 and m_2, and an internal rotor with mass m_r and central moment of inertia I_r. The motion of the internal masses is bounded by the body's shell and is performed along smooth trajectories $\boldsymbol{\rho}_1 = (\xi_1(t),\, \eta_1(t))$ and $\boldsymbol{\rho}_2 = (\xi_2(t),\, \eta_2(t))$. The material point m_i models a cam if the curve $\boldsymbol{\rho}_i$ is a circle, and m_i models a slider if $\boldsymbol{\rho}_i$ is a straight line. The rotor has a circular shape, rotates with angular velocity $\Omega(t)$, its axis of rotation is perpendicular to the plane of motion and passes through the center of mass of the rotor. To describe the motion of the body, let us introduce two Cartesian coordinate systems: a fixed one, Oxy, and a moving one, $O_1\xi\eta$, attached to the body (see Fig. 1). Point O_1 concides with the position of the center of mass of the body-rotor system. The center of mass of the body is denoted by O_b and the center of mass of the rotor is denoted by O_r. For the system under consideration the following kinematic relations hold [2, 3]:

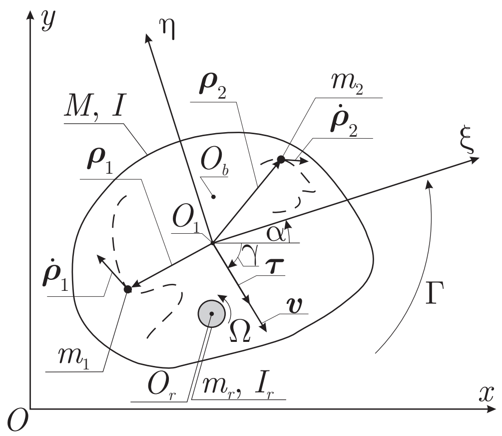

Fig. 1. A rigid body with two internal masses and internal rotor

$$\dot{x} = v_1 \cos\alpha - v_2 \sin\alpha, \quad \dot{y} = v_1 \sin\alpha + v_2 \cos\alpha, \quad \dot{\alpha} = \omega, \tag{1}$$

where x and y are the coordinates of the point O_1 in absolute space, α is the angle of rotation of the body, v_1, v_2 are the components of the velocity of the body referred to the axes of the moving coordinate system, and ω is the angular velocity of the body.

The equations of motion of the body can be written in the form of Poincaré equations on the group $E(2)$ [2, 3]

$$\begin{gathered}
\frac{d}{dt}\left(\frac{\partial L}{\partial v_1}\right) = \omega\frac{\partial L}{\partial v_2} + \cos\alpha\frac{\partial L}{\partial x} + \sin\alpha\frac{\partial L}{\partial y},\\
\frac{d}{dt}\left(\frac{\partial L}{\partial v_2}\right) = -\omega\frac{\partial L}{\partial v_1} - \sin\alpha\frac{\partial L}{\partial x} + \cos\alpha\frac{\partial L}{\partial y},\\
\frac{d}{dt}\left(\frac{\partial L}{\partial \omega}\right) = v_2\frac{\partial L}{\partial v_1} - v_1\frac{\partial L}{\partial v_2} + \frac{\partial L}{\partial \alpha}
\end{gathered} \tag{2}$$

with Lagrangian

$$L = \frac{1}{2}\left(\mathbf{A}\boldsymbol{w},\, \boldsymbol{w}\right) + \left(\boldsymbol{c},\, \boldsymbol{w}\right) + \left(\boldsymbol{u},\, \boldsymbol{w}\right), \tag{3}$$

where

$$\mathbf{A} = \begin{pmatrix} a_1 & 0 & f \\ 0 & a_2 & g \\ f & g & b \end{pmatrix}, \quad \boldsymbol{u} = \begin{pmatrix} m_1\dot{\xi}_1 + m_2\dot{\xi}_2 \\ m_1\dot{\eta}_1 + m_2\dot{\eta}_2 \\ m_1\left(\xi_1\dot{\eta}_1 - \dot{\xi}_1\eta_1\right) + m_2\left(\xi_2\dot{\eta}_2 - \dot{\xi}_2\eta_2\right) + I_r\Omega \end{pmatrix}$$

$$\boldsymbol{w} = \begin{pmatrix} v_1 \\ v_2 \\ \omega \end{pmatrix}, \quad \boldsymbol{c} = \begin{pmatrix} -\frac{\lambda}{2}\left(x\sin\alpha - y\cos\alpha\right) \\ -\frac{\lambda}{2}\left(x\cos\alpha + y\sin\alpha\right) \\ -\chi\left(x\sin\alpha - y\cos\alpha\right) - \zeta\left(x\cos\alpha + y\sin\alpha\right) \end{pmatrix}$$

$$a_1 = M + m_1 + m_2 + m_r + \lambda_1, \quad a_2 = M + m_1 + m_2 + m_r + \lambda_2,$$

$$b = M\left(\xi_b^2 + \eta_b^2\right) + m_1\left(\xi_1^2 + \eta_1^2\right) + m_2\left(\xi_2^2 + \eta_2^2\right) + m_r\left(\xi_r^2 + \eta_r^2\right) + I + I_r + \lambda_6,$$

$$f = -m_1\eta_1 - m_2\eta_2, \quad g = m_1\xi_1 + m_2\xi_2.$$

Here $\lambda = \rho\Gamma$, $\zeta = \rho\Gamma\nu$, $\chi = \rho\Gamma\mu$, ρ is the density of the fluid, μ, ν are the coefficients associated with the hydrodynamic asymmetry of the body [1], λ_1, λ_2 are the added masses, and λ_6 is the added moment of inertia.

Equations (1) and (2) admit the following first integrals [2]:

$$\begin{aligned} p_x &= \left(\frac{\partial L}{\partial v_1} - \chi\right)\cos\alpha - \left(\frac{\partial L}{\partial v_2} - \zeta\right)\sin\alpha + \frac{\lambda}{2}y, \\ p_y &= \left(\frac{\partial L}{\partial v_1} - \chi\right)\sin\alpha + \left(\frac{\partial L}{\partial v_2} - \zeta\right)\cos\alpha - \frac{\lambda}{2}x, \\ K &= xp_y - yp_x + \frac{\partial L}{\partial \omega} + \frac{\lambda}{2}\left(x^2 + y^2\right) - c_3. \end{aligned} \tag{4}$$

At a zero value of circulation the controllability is proved for various combinations of control elements (two cams, cam and rotor, slider and rotor). For the case of two cams, elementary controls providing rotation and motion which is on the average rectilinear have been contructed.

The analysis of the free motion is performed at nonzero value of circulation. The controllability is proved for various control systems (single rotor, arbitrary moving internal mass, cam and rotor, slider and rotor). It is shown that a drift occurs in the presence of circulation. The drift implies motion of the body without control. Controls providing a partial compensation of the drift are derived.

References

[1] Chaplygin S.A. On the influence of a plane-parallel flow of air on moving through it a cylindrical wing // Tr. Cent. Aerohydr. inst. 1926. Vyp. 19. pp. 300–382

[2] Borisov A.V., Mamaev I.S. Rigid body dynamics. Hamiltonian methods, integrability, chaos, MoscowIzhevsk: Institute of Computer Science, 2005, 576 pp.

[3] Vetchanin E. V., Kilin A. A., Free and controlled motion of a body with moving internal mass though a fluid in the presence of circulation around the body, Doklady Physics, 2016, vol. 466, no. 3, pp. 293-297

Analysis of the influence of the rolling friction on the dynamics of a robot-wheel

Alexander Kilin[1], Anton Klekovkin[2] and Elena Pivovarova[1]

[1] *Udmurt State University, Izhevsk, Russia*
[2] *M. T. Kalashnikov Izhevsk State Technical University, Izhevsk, Russia*

In this work we consider the dynamics of a robot-wheel moving by changing the proper gyrostatic momentum (by using a controlled gyrostat) on a plane in the presence of rolling friction (see Fig. 1). The problem is considered under the assumption that the center of mass of the system does not coincide with its geometrical center. Equations of motion describing the dynamics of the system are derived and the controlled motion (controlled acceleration and deceleration during the motion in a straight line) of the wheel is considered by giving the constant angular acceleration of the rotor (gyrostat).

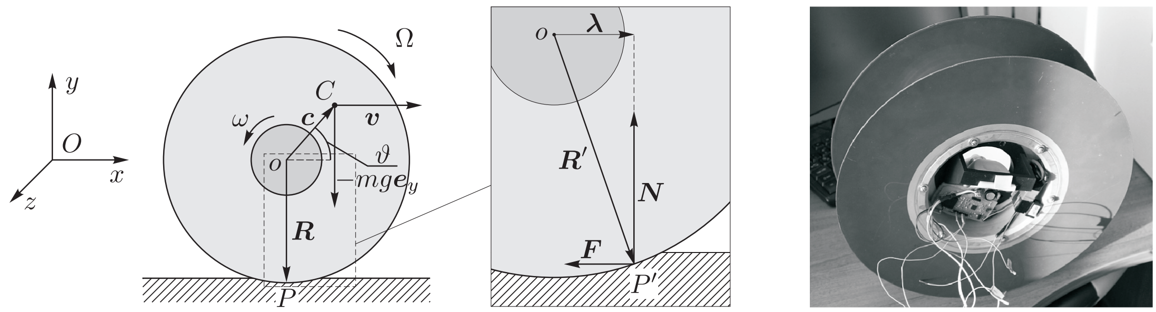

Figure 1. Model of a robot-wheel and photograph of the full-scale specimen.

To prove the applicability of the proposed mathematical model, we develop experimental methods for investigating the dynamics of the system in the presence of rolling friction and we conduct experimental research on the controlled motion of the robot-wheel. Theoretical data and experimental results are compared. It is shown that the theoretical results are in a good qualitative agreement with the experimental results, but are quantitatively different.

To reduce this difference, we consider several models of rolling friction that take into account nonuniformity of the coefficient of rolling friction and its dependence on the linear velocity.

Precession on a rotating saddle: a gyro force in an inertial frame

Oleg N. Kirillov[1], Mark Levi[2]

[1] *Russian Academy of Sciences, Steklov Mathematical Institute, Moscow, Russia*
[2] *Department of Mathematics, Pennsylvania State University, University Park, USA.*

The existence of Trojan asteroids in a triangular Lagrange libration point on the orbit of Jupiter is a consequence of the basic fact that a particle can be trapped in the rotating saddle potential. In the case when the potential is symmetric, the trajectory of the trapped particle in the non-rotating frame exhibits a slow prograde precession. This somewhat mysterious precession discovered first in the context of accelerator physics and microwave ion traps has not been explained so far. We demonstrated that the rapid rotation of the saddle potential creates a weak Lorentz-like (or Coriolis-like) force, in addition to an effective stabilizing potential, all in the inertial frame. With the use of a new hodograph transformation and a method of normal form, we found a simplified equation for the guiding center of the trajectory that coincides with the equation of the Foucault's pendulum. In this sense, a particle trapped in the symmetric rotating saddle trap is, effectively, a Foucault's pendulum, but in the inertial frame.

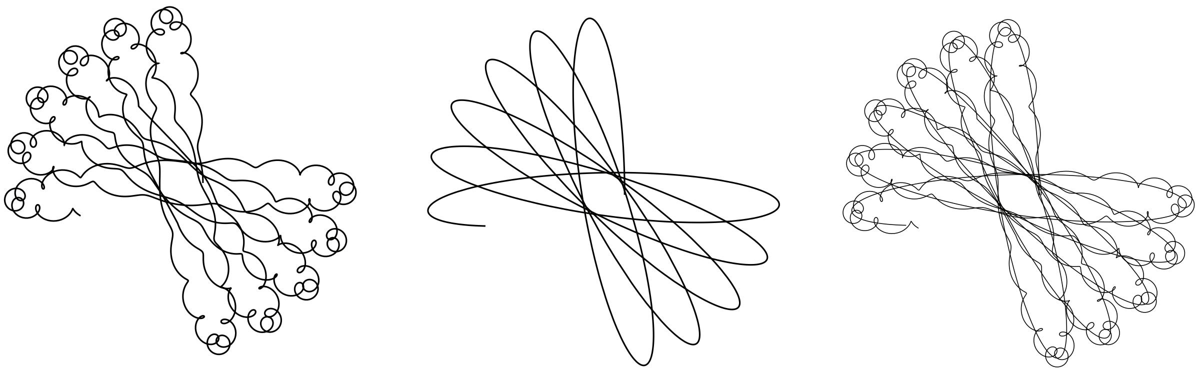

Fig. 1. A typical trajectory of a particle trapped by a symmetric rotating saddle (in the stationary frame); its guiding center; their superposition.

References

[1] Brouwer L.E.J. *Beweging van een materieel punt op den bodem eener draaiende vaas onder den invloed der zwaartekracht* // Nieuw Archief voor Wiskunde, 1918, vol. 2, pp. 407–419.

[2] Bialynicki-Birula I., Kaliński M., Eberly J.H. *Lagrange equilibrium points in celestial mechanics and nonspreading wave packets for strongly driven Rydberg electrons* // Physical Review Letters, 1994, vol. 73, 1777–1780.

[3] Shapiro V.E., *The gyro force of high-frequency fields lost by the concept of effective potential* // Physics Letters A, 1998, vol. 238, 147–152.

[4] Bialynicki-Birula I., Bialynicka-Birula Z., Chmura B. *Trojan states of electrons guided by Bessel beams* // Laser Physics, 2005, vol. 15, no. 10, pp. 1371–1380.

[5] Kirillov O.N., Levi M. *Rotating saddle trap as Foucault's pendulum* // American Journal of Physics, 2016, vol. 84, no. 1, pp. 26–31.

Model development of a screwless underwater robot

Anton V. Klekovkin[1], Ivan S. Mamaev[2]

[1] *Izhevsk State Technical University, ul. Studencheskaya, 7, Izhevsk, 426069 Russia*
[2] *Udmurt State University, ul. Universitetskaya, 1, Izhevsk, 426034 Russia*

This work devoted to creation of underwater robot which moves using internal rotors. The developed design of underwater robot has no moving elements interacting with environment. This feature minimizes a negative influence on environment and ensures noiseless of robot movement in fluid.

Despite many discussions about possibility and effectiveness of moving using shift of internal masses, many last published articles confirm research relevance [1-6]. The moving possibility of a body on plane using rotors is demonstrated in paper [7]. The results of experimental investigation of movement by means of gaits for internal rotor are presented in [8]. Also, the feasibility of this type of motion is shown in practice. The equations of moving body which has 3 internal rotors in ideal fluid are given in paper [9].

In this paper we suggest the design of screwless underwater robot moving by rotation of internal rotors for theoretical and experimental investigations.

For experimental research we designed the model of underwater robot that consist of hollow ellipsoid and 3 internal rotors which have orthogonal axes. The center of mass of the system coincides with geometrical center of ellipsoid. The equations of motion are given in the form of classical Kirchhoffs equations. The control is realized by change of rotation speed of internal rotors, which are set in motion by direct current motors.

References

[1] Volkova L.Yu., Yatsun S.F. *Control of the three-mass robot moving in the liquid environment* // Nelin. Dinam, 2011, vol. 7, no. 4, pp. 845–857.

[2] Borisov A.V., Mamaev I.S., Kilin A.A., Kalinkin A.A., Karavaev Yu. L., Klenov A.I., Vetchanin E.V., Tenenev V.A. *Bezvintovoi nadvodnyi robot (Screwless above-water robot)* // Patent RF, no. 153711, 2015.

[3] Ramodanov S.M., Tenenev V.A. *Motion of a body with variable distribution of mass in a boundless viscous liquid* // Nelin. Dinam, 2011, vol. 7, no. 3, pp. 635–647.

[4] Vetchanin E.V., Tenenev V.A. *Motion control simulating in a viscous liquid of a body with variable geometry of weights* // Komp'yuternye issledovaniya i modelirovanie, 2011, vol. 3, no. 4, pp. 371–381.

[5] Vetchanin E.V., Mamaev I.S., Tenenev V.A. *The motion of a body with variable mass geometry in a viscous fluid* // Nelin. Dinam, 2012, vol. 8, no. 4, pp. 815–836.

[6] Vetchanin E.V., Kilin A.A. *Free and controlled moving body with mobile internal mass in fluid with circulation around body* // Doklady mathematics, 2016, vol. 466, no. 3, pp. 293–297.

[7] Borisov A.V., Kilin A.A., Mamaev I.S. *How to Control the Chaplygin Ball Using Rotors. II* // Regular and Chaotic Dynamics, 2013, vol. 18, no. 1-2, pp. 144–158.

[8] Kilin A.A., Karavaev Yu. L. *Experimental research of dynamic of spherical robot of combined type* // Nelin. Dinam, 2015, vol. 11, no. 4, pp. 721–734.

[9] Vetchanin E. V., Karavaev Yu. L., Kalinkin A. A., Klekovkin A. V., Pivovarova E. N. *Model of screwless underwater robot* // Vestnik Udmurtskogo universiteta. Matematika. Mehanika. Komp'yuternye nauki, 2015, vol. 25, no. 4, pp. 544–553.

Theoretical and experimental investigation of the motion of a screwless overwater mobile platform

Anatoliy I. Klenov[1,2], Eugenii V. Vetchanin[1,2]

[1] *Kalashnikov Izhevsk State Technical University, Izhevsk, Russia.*
[2] *Udmurt State University, Izhevsk, Russia*

Currently, water mobile platforms are widely used for monitoring the state of the aquatic environment, taking water samples, and others. Sometime it is needed devices that don't strongly affect the processes of a medium under investigation. Using a screwless vehicle in similar applications has a number of constructive and operational advantages: isolation of the operating units from the liquid, simple design, maneuverability, increased environmental friendliness.

This work is concerned with investigation of the motion of a screwless overwater platform, moving by means of the change of the center mass of the system. This change is performed by use of two rotating internal masses. The theoretical possibility of this method of motion has been proved in [1, 2]. In this paper the results of theoretical and experimental study of the motion of the screwless overwater platform are presented. The theoretical study is performed within the framework of theory of an ideal fluid. The experimental study includes determinining the added masses and the added moment of inertia by the method of towing ([3]), PIV measurements of the velocity field of the fluid around the moving platform, and determining the trajectory of motion of the body by using a Motion Capture System.

References

[1] Kozlov V. V., Ramodanov S. M. *On the motion of a body with a rigid hull and changing geometry of masses in an ideal fluid*// Report Russian Academy of Sciences. 2002, vol. 382, no.4, pp. 478-481.

[2] Kilin A. A., Vetchanin E. V. *The contol of the motion through an ideal fluid of a rigid body by means of two moving masses.*// Nonlinear dynamics, 2015, vol. 11, no. 4, pp. 633 - 645.

[3] Klenov A. I., Vetchanin E. V., Kilin A. A., *Experimental determination of the added mass of the body by towing*// Vestnik Udmurtskogo Universiteta, 2015, vol. 25, no. 4, pp. 568 - 582.

Integrability of the Liénard–type equations and non–local transformations

Nikolay A. Kudryashov[1], Dmitry I. Sinelshchikov[1]

[1] *Department of Applied Mathematics, National Research Nuclear University MEPhI, Moscow, Russian Federation*

In this talk we consider the following family of the Liénard–type equations

$$y_{zz} + f(y)y_z^2 + g(y)y_z + h(y) = 0, \tag{1}$$

where $f(y)$, $g(y)$ and $h(y)$ are arbitrary functions. We suppose that functions $f(y)$ and $g(y)$ do not vanish simultaneously. In the case of $f(y) = 0$ we have the classical Liénard equation, while for $g(y) = 0$ we obtain the quadratic Liénard equation. In the general case, i.e. when $f(y) \neq 0$ and $g(y) \neq 0$, equation (1) is called mixed Liénard–type equation. Equation (1) has a vast range of application in physic, mechanics, biology e.t.c. (see, e.g. [1, 2, 3]). For example, some famous nonlinear oscillators and planar dynamical systems, such as the Rayleigh equation for bubble dynamics and the Van–der Pol equation, belong to family of equations (1). Traveling–wave reduction of some nonlinear partial differential equations, for instance the Camass–Holm and the K(m,n) equation, are also members of family of equations (1).

Although family of equations (1) has been intensively studied for several past decades a question about constructing general analytical solutions of this equation has not been completely answered yet. In this talk we discuss an approach for finding integrable subclasses of equation (1) that has been recently proposed in works [4, 5]. The main idea of this approach is to study connections between equation (1) and other nonlinear differential equations, which can be analytically solved. It is supposed that these connections are given by nonlocal transformations that are generalization of the Sundman transformations (see, e.g. [6, 7]). These transformations have the form

$$w = F(y), \quad d\zeta = G(y)dz, \quad F_y G \neq 0 \tag{2}$$

where w and ζ are new dependent and independent variables correspondingly.

First of all, we consider the quadratic Liénard equation i.e. equation (1) with $g(y) = 0$. We show that with the help of the generalized Sundman transformations this equation can be transformed into an equation for the elliptic function for arbitrary functions $f(y)$ and $h(y)$. Therefore, the general solution of (1) with $g(y) = 0$ can be expressed in terms of the elliptic functions for arbitrary functions $f(y)$ and $h(y)$. We illustrate our results by constructing several new generals solutions of both some two–dimensional dynamical systems and traveling–wave reductions of some nonlinear partial differential equations.

Then we study the classical Liénard equation, that is equation (1) with $f(y) = 0$. By studying connections between the classical Liénard equation and some equations of the Painlevé–Gambier type, which are subcases of (1) at $f(y) = 0$, we obtain new criteria for the integrability of the former equation. In other words, we found correlations on functions $g(y)$ and $h(y)$ that allow us to construct the general analytical solutions of the corresponding classical Liénard equations. We demonstrate effectiveness of our approach by constructing several new integrable Liénard equations along with their general solutions.

Finally, we discuss integrability of equation (1) in the case of $f(y) \neq 0$ and $g(y) \neq 0$. It is worth noting that in this case equation (1) can be mapped into equation (1) with $f(y) = 0$. Therefore, we can use criteria for the integrability of the classical Liénard equation for finding integrable mixed Liénard–type equations. On the other hand, we can look for new integrability criteria for the mixed Liénard–type equations with the help of the connections between these equations and some subcases of equation (1) with $f(y) \neq 0$ and $g(y) \neq 0$ that are of the Painlevé–Gambier type. As a result, we find some new integrability criteria for the mixed Liénard–type equations. These criteria can also be used as criteria for the integrability of the classical Liénard equation since this equation is connected to equation (1) via (2). We demonstrate applications of our approach by constructing several examples of the integrable mixed Liénard–type equations.

This work was partially supported by grant for the state support of young Russian scientists 6624.2016.1 and by RFBR grant 140100498.

References

[1] Guckenheimer J., Holmes P. *Nonlinear Oscillations, Dynamical Systems, and Bifurcations of Vector Fields.* Springer New York, 1983, 462 p.

[2] Andronov A. A., Vitt A. A., Khaikin S. E. *Theory of Oscillators.* Dover Publications, New York, 2011, 864 p.

[3] Zaitsev V. F., Polyanin A. D. *Handbook of Exact Solutions for Ordinary Differential Equations.* Chapman and Hall/CRC, Boca Raton, 2002, 816 p.

[4] Kudryashov N. A., Sinelshchikov D. I. *On the connection of the quadratic Lienard equation with an equation for the elliptic functions.* Regul. Chaotic Dyn., 2015, vol. 20, pp. 486–496.

[5] Kudryashov N. A., Sinelshchikov D. I. *On the criteria for integrability of the Linard equation.* Appl. Math. Lett., 2016, vol. 57, pp. 114–120.

[6] Nakpim W., Meleshko S. V. *Linearization of Second-Order Ordinary Differential Equations by Generalized Sundman Transformations.* Symmetry, Integr. Geom. Methods Appl., 2010, vol. 6, pp. 1–11.

[7] Moyo S., Meleshko S. V. *Application of the generalised Sundman transformation to the linearisation of two second-order ordinary differential equations.* J. Nonlinear Math. Phys., 2011, vol. 18, pp. 213–236.

Modern Lyapunov analysis: Covariant Lyapunov vectors and structure of invariant manifolds of chaotic attractors

Pavel V. Kuptsov[1]

[1] *Institute of electronics and mechanical engineering, Yuri Gagarin State Technical University of Saratov, Saratov, Russia*

Until the recent times practically applicable Lyapunov analysis of nonlinear systems contained only the concept of Lyapunov exponents accompanied by the algorithm reported by Benettin et al. [1] and by Shimada and Nagashima [2]. However it was known that there exist special vectors that are tangent to expanding and contracting manifolds of trajectories and whose growth (or decay) exponents are the Lyapunov exponents [3]. These vectors has became available when two groups reported simultaneously and independently two different algorithms for their computations [4, 5].

Significant progress in applications of covariant Lyapunov vectors has been achieved in computation of angles between invariant manifolds for numerical verification of hyperbolicity of chaotic dynamics. Based on the detailed analysis of the vectors computation routines [6], an effective algorithm has been derived that admits the verification of hyperbolicity even for high dimensional systems [7].

In this talk we review the methods of computation of covariant Lyapunov vectors as well as the corresponding angles and represent the recent results on extension of these methods to time-delay systems [8].

References

[1] Benettin G., Galgani L., Giorgilli A., Strelcyn, J.-M. *Lyapunov Characteristic Exponents for smooth dynamical systems and for hamiltonian systems: a method for computing all of them. Part 1: Theory* // Meccanica, 1980, vol 15, no. 1, pp. 9–20.

[2] Shimada I., Nagashima T. *A numerical approach to ergodic problem of dissipative dynamical systems* // Prog. Theor. Phys., 1979, vol. 6, no. 6, pp. 1605–1616.

[3] Eckmann J. P., Ruelle D. *Ergodic theory of chaos and strange attractors* // Rev. Mod. Phys., 1985, vol. 57, no. 3, pp. 617–656.

[4] Ginelli, F., Poggi, P., Turchi, A., Chaté, H., Livi, R., Politi, A. *Characterizing dynamics with covariant Lyapunov vectors* // Phys. Rev. Lett., 2007, vol. 99, p. 130601.

[5] Wolfe, C. L., Samelson, R. M. *An efficient method for recovering Lyapunov vectors from singular vectors* // Tellus A, 2007, vol. 59, pp. 355–366.

[6] Kuptsov, P. V., Parlitz, U. *Theory and Computation of Covariant Lyapunov Vectors* // J. Nonlinear. Sci., 2012, vol. 22, no. 5, pp. 727–762.

[7] Kuptsov, P. V. *Fast numerical test of hyperbolic chaos* // Phys. Rev. E, 2012, vol. 85, p. 015203.

[8] Kuptsov, P. V., Kuznetsov S. P. *Numerical test for hyperbolicity of chaotic dynamics in time-delay systems* // arXiv:1604.03521, 2016.

Reconstruction of model equations to the problem of the body of elliptic cross-section falling in a viscous fluid

Sergey P. Kuznetsov[1,3], Alexey V. Borisov [1], Ivan S. Mamaev [1,2] and Valentin A. Tenenev [2]

[1] *Udmurt State University, Izhevsk, Russia*
[2] *Izhevsk State Technical University, Russia*
[3] *Institute of Radio-Engineering and Electronics of RAS, Saratov Branch, Russia*

By processing time series obtained from numerical solution of the plane problem for the motion of a body of elliptic cross-section with gravity in incompressible viscous fluid, a system of ordinary differential equations is reconstructed for approximate description of the dynamics. The postulated equations take into account the added masses, the force caused by the circulation of the velocity field, and the movement resistance forces, and the coefficients in these equations are evaluated using the least squares method to fit the observable time series data. Correspondence is illustrated of the finite-dimensional description and simulation based on the Navier – Stokes equations by portraits of attractors in regular and chaotic regimes. Moreover, the obtained coefficients provide a glimpse of the real contribution of various effects in the body dynamics.

The model equations in dimensionless variables are of the form

$$A\dot{u} = Bvw - Dvw - C|u|u - \sin\theta, \quad B\dot{v} = -Auw + Duw - E|v|v - \cos\theta,$$
$$\dot{w} = -Guv - H|w|w, \quad \dot{\theta} = w, \tag{1}$$

$$\dot{X} = u\cos\theta - v\sin\theta, \ \ \dot{Y} = u\sin\theta + v\cos\theta. \tag{2}$$

The coefficients obtained by processing the results of the numerical solution of two-dimensional problem of the fall of the body of elliptic profile for the semi-axes a=0.486 cm and $b = a$/6=0.081 cm, viscosity η=0.001 Pa×s, fluid density ρ_f=1000 kg / m^3 are listed in the Table for variants with different densities of the body ρ_s.

ρ_s, kg/m^3	1710	2000	2300	2600	2900	3600
A	1.3945	1.3392	1.2581	1.1975	1.1551	1.0388
B	4.7378	3.9290	3.2845	2.7320	2.3245	1.9196
C	0.1069	0.0891	0.0873	0.0850	0.1209	0.1044
D	1.9730	1.8751	1.7952	1.6617	1.6221	1.2957
E	1.7720	1.5770	1.3803	1.3248	1.1254	0.7034
G	0.8681	0.8665	0.8516	0.7893	0.7710	0.5636
H	0.4130	0.3884	0.3163	0.2723	0.2775	0.0073

Figure 1 compares the trajectories of the fall resulting from a two-dimensional numerical solution of the problem with Navier – Stokes equations and within the finite-dimensional model (1), (2). Figure 2 compares portraits of attractors in the projection on the plane of the variables for the same modes.

Thus, in this report we have demonstrated a possibility of rather satisfactory approximate description of the motion of the body of elliptical cross-section under gravity in a fluid using ordinary differential equations reconstructed on the basis of the processing data from the numerical solution of the problem with the Navier – Stokes equations. The proposed approach is interesting, in particular, in relation to the control problems concerning motions of bodies in fluid as the description is much easier than the rigorous computations while the degree of quantitative compliance is better than that in the previously discussed phenomenological models.

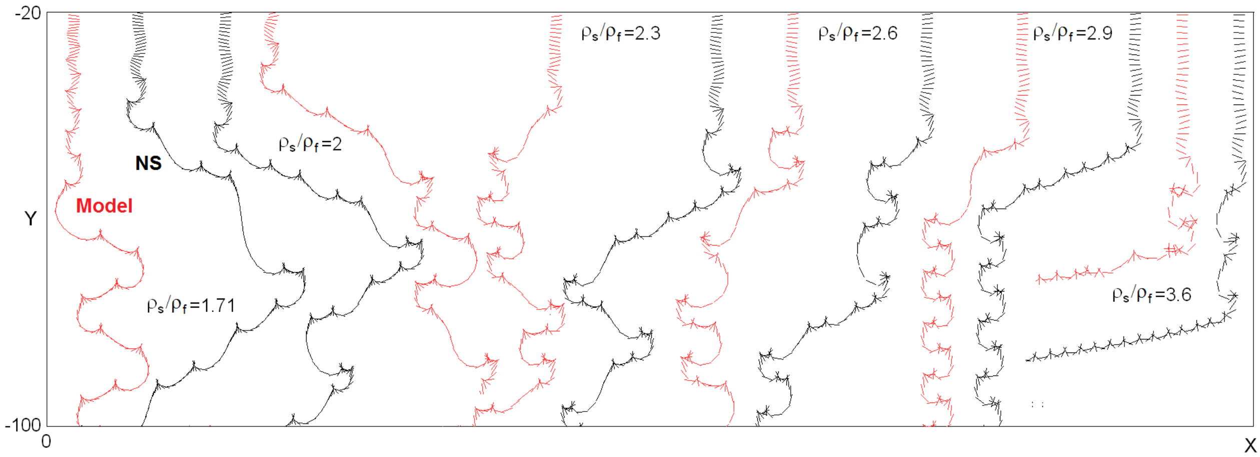

Fig. 1. Stroboscopic visualization of the body falling in a fluid: instant positions of the major axis of the ellipse at successive time points are shown based on the results of numerical simulation with the Navier – Stokes (NS) and obtained for the model (1), (2) with coefficients from the Table.

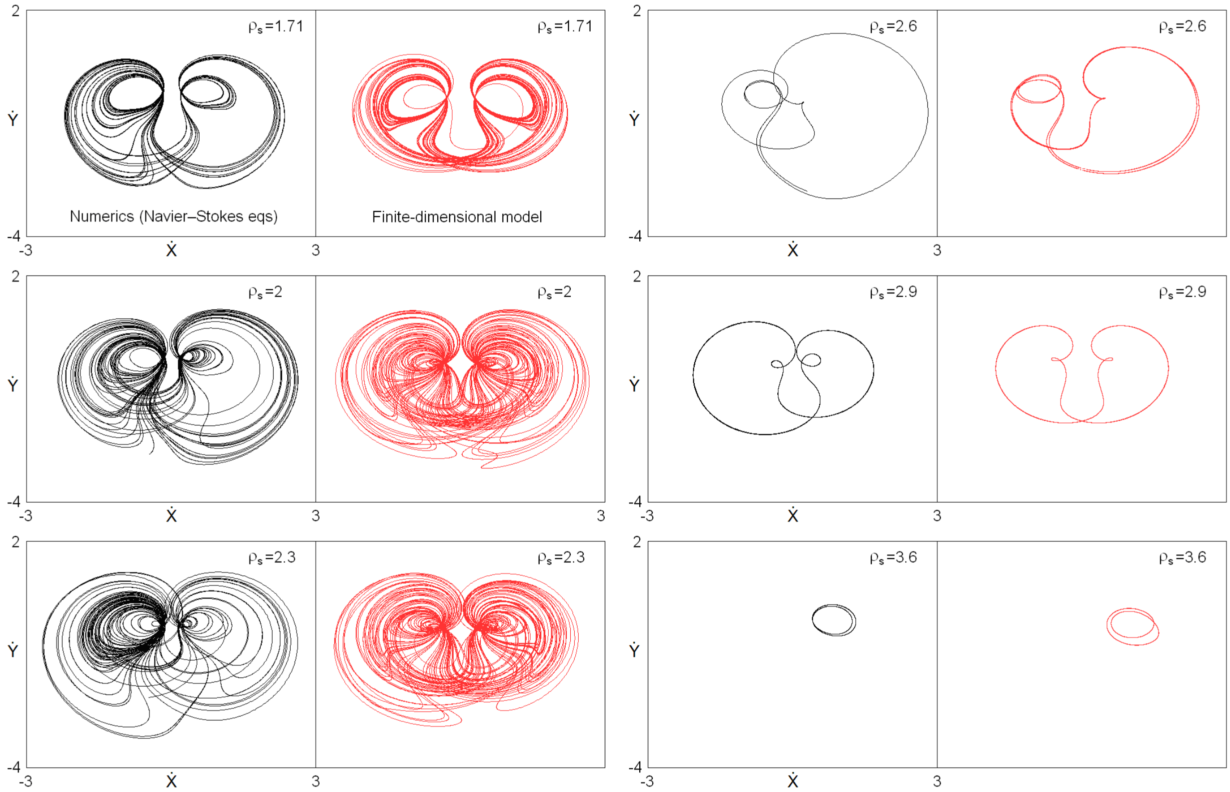

Fig. 2. Portraits of attractors in projection onto a plane $(\dot{X},\ \dot{Y})$ from numerical simulation of the dynamics with the Navier – Stokes equations (left columns) and from the model (1), (2) (right columns) for different body densities.

Elaboration of the finite-dimensional model and computations on its base were supported by RSF grant No 15-12-20035. Computations based on the Navier – Stokes equations to obtain data for the model reconstructions were carried out under support of the RSF grant No 14-19-01303.

Slow-fast dynamics of a Duffing type equation: a case of study

Lev Lerman[1], Alexey Kazakov[1] and N.Kulagin[2]

[1] *Lobachevsky State University of Nizhny Novgorod, Nizhny Novgorod, Russia*
[2] *Moscow Aviation Institute, Moscow, Russia*

As a representative example of a periodic in time Hamiltonian system in one degree of freedom with a slow varying parameter we study a system of the Duffing type

$$\dot{x} = y,\ \dot{y} = -\sin\theta - x\cos\theta - x^3,\ \dot{\theta} = \varepsilon \tag{1}$$

with Hamiltonian

$$H = \frac{y^2}{2} + \frac{x^4}{4} + \frac{x^2}{2}\cos\theta + x\sin\theta.$$

This systems demonstrates all types of the orbit behavior possible for a one and a half degree of freedom Hamiltonian system. The goal of the talk is to explain this behavior using the tools available by now in the theory of two dimensional symplectic diffeomorphisms. Of course, it is not possible to present completely rigorous explanations of the chaotic behavior observed in the system. No tools exist nowadays that allow to give a more or less satisfactory picture of the motion in the chaotic zones for a smooth symplectic 2-dimensional diffeomorphism.

The system under the study is rather simple in its form, it is reversible in the phase space $\mathbf{R^2}\times\mathbf{S^1}$ and has a minimally possible number of degenerate equilibria of simplest type (parabolic ones) for the frozen (fast) systems.

This study allowed us to find for the related Poincaré map:

1. The region where there is an eternal adiabatic invariant;

2. A disk-shaped region where the dynamics is chaotic, Lyapunov exponent calculated numerically have appeared positive, this region has infinitely many hyperbolic periodic orbits with the homo- heterocilic tangles;

3. Existence of relaxation symmetric periodic orbits which some finite time pass near unstable hyperbolic part of the slow curve, like for canard periodic orbits;

4. Infinitely many bifurcations of symmetric periodic orbits of different types.

To investigate the dynamics we use various tools: the results on the almost integrable normal form for the Hamiltonian near its almost elliptic slow curve, the Fenichel results on the existence of hyperbolic slow manifold, blow up technique to represent the orbit transition near the disruption points, for the case of Hamiltonian system this is intimately connected with different solutions of the Painlevé-I equation. The talk is based on the results of the paper [1].

References

[1] Kazakov A., Kulagin N., Lerman L. *Relaxation oscillations and chaos in a Duffing type equation: a case study*, 2016, submitted to Discontinuity, Nonlinearity, Complexity

On nilpotent approximations of non-smooth Hamiltonian systems

Lev Lokutsievskiy[1]

[1] *Lomonosov Moscow State University, Moscow, Russia*

I plan to discuss a new approach to study non-smooth Hamiltonian systems. Namely, this approach is based on the fact that nilpotent approximations of such systems are nilpotent-convex problems of optimal control. The optimal synthesis in these problems forms a half flow on the phase space and hence can be studied from three different points of view: by methods of dynamical systems, by topological methods and by methods of convex analysis. This half flow has many nice properties and some of them can be restored in the original non-smooth Hamiltonian system. This approach gives very powerful results when the half flow in the corresponding nilpotent-convex problem has chaotic nature. Another interesting corollary comes from the Lefschetz formula which allows to prove existence of periodic trajectories of special kind.

Dynamics of chains in external fields

Andrzej J. Maciejewski [1] and Maria Przybylska[2]

[1] *Janusz Gill Institute of Astronomy, University of Zielona Góra, Poland*
[2] *Institute of Physics, University of Zielona Góra, Poland*

We discusses the dynamics of systems of point masses joined by massless rigid roods in the field of a potential force. General form of equations of motion for such systems is obtained. We investigate integrability of these equations in a case when the chain moves in constant and linear field of forces. Moreover, the dynamics of a linear chain of mass points moving around a central body in an orbit is analysed. The non-integrability of the chain of three masses moving in circular Kepler orbit around a central body is proven. This was achieved thanks to an analysis of variational equations along two particular solutions and an investigation of their differential Galois groups.

Integrability obstructions of certain homogeneous Hamiltonian systems in 2D curved spaces

Andrzej J. Maciejewski[1], Maria Przybylska[2], Wojciech Szumiński[2]

[1] *J. Gil Institute of Astronomy, University of Zielona Góra, Poland*
[2] *Institute of Physics, University of Zielona Góra, Poland*

Integrability of natural Hamiltonian systems of the form

$$H = \frac{1}{2}\sum_{i=1}^{n} p_i^2 + V(\boldsymbol{q}), \qquad \boldsymbol{q} = (q_1, \ldots, q_n), \tag{1}$$

has been intensively investigated during last decades and significant successes were achieved. Here $\boldsymbol{q} = (q_1, \ldots, q_n)$ and $\boldsymbol{p} = (p_1, \ldots, p_n)$ are canonical variables in $\mathbb{C}^{2n}$ considered as a symplectic linear space. It seems that among new methods which have been invented, the most powerful and efficient are those formulated in the framework of the differential Galois theory. The necessary conditions for the integrability of a Hamiltonian system in the Liouville sense are given in terms of properties of the differential Galois group of variational equations obtained by linearisation of equations of motion in a neighbourhood of a particular solution. The fundamental Morales-Ramis theorem of this approach says that if a Hamiltonian system is meromorphically integrable in the Liouville sense in a neighbourhood of a phase curve $\boldsymbol{\Gamma}$ corresponding to a particular solution, then the identity component $\mathcal{G}^0$ of the differential Galois group $\mathcal{G}$ of variational equations along $\boldsymbol{\Gamma}$ is Abelian, see e.g. [5].

This approach has been appeared especially successful for the case when potential $V(\boldsymbol{q})$ is a homogeneous function of variables $\boldsymbol{q}$ of degree $k \in \mathbb{Z}$. While it can be not easy to find a particular solution necessary for the application the differential Galois methods, for Hamilton systems (1) with homogeneous potential $V(\boldsymbol{q})$ some particular solutions can be constructed in a systematic way. They are built by means of a non-zero solution $\boldsymbol{d} \in \mathbb{C}^n$ of the non-linear system $V'(\boldsymbol{d}) = \boldsymbol{d}$. Moreover, variational equations along these particular solutions can be transformed into a system of uncoupling hypergeometric equations depending on the degree of homogeneity k and eigenvalues λ_i, for $i = 1, \ldots, n$, of the Hessian $V''(\boldsymbol{d})$. Since differential Galois group of the hypergeometric equation is well known it was possible to obtain necessary conditions of the integrability of Hamilton systems (1) in the form of arithmetic restrictions on λ_i that must belong to appropriate sets of rational numbers depending on k, see e.g. [5]. Later it appeared that between λ_i some universal relations exist which improves conditions mentioned in the above papers e.g. [2, 6].

Successful integrability analysis of Hamiltonian systems with homogeneous potentials in flat Euclidean spaces motivated us to look for systems in curved spaces with similar properties. We propose two classes of Hamiltonians. The first class of Hamiltonian systems is governed by

$$H = T + V, \qquad T = \frac{1}{2}r^{m-k}\left(p_r^2 + \frac{p_\varphi^2}{r^2}\right), \qquad V = r^m U(\varphi), \tag{2}$$

where m and k are integers, $k \neq 0$ and $U(\varphi)$ is a meromorphic function. If we consider (r, φ) as the polar coordinates, then the kinetic energy corresponds to a singular metric on a plane or a sphere. This is just an example of a natural system which possesses certain common features with standard systems with homogeneous potentials in the Euclidean plane $\mathbb{E}^2$.

The second class of natural Hamiltonian systems with two degrees of freedom is defined on $T^\star M^2$ where M^2 is a two dimensional manifold with a constant curvature metrics. Manifold M^2

is either sphere $\mathbb{S}^2$, the Euclidean plane $\mathbb{E}^2$, or the hyperbolic plane $\mathbb{H}^2$. In order to consider those three cases simultaneously we will proceed as e.g. in [1] and we define the following functions

$$\mathrm{C}_\kappa(x) := \begin{cases} \cos(\sqrt{\kappa}x) & \text{for} \quad \kappa > 0, \\ 1 & \text{for} \quad \kappa = 0, \\ \cosh(\sqrt{-\kappa}x) & \text{for} \quad \kappa < 0, \end{cases} \tag{3}$$

$$\mathrm{S}_\kappa(x) := \begin{cases} \frac{1}{\sqrt{\kappa}}\sin(\sqrt{\kappa}x) & \text{for} \quad \kappa > 0, \\ x & \text{for} \quad \kappa = 0, \\ \frac{1}{\sqrt{-\kappa}}\sinh(\sqrt{-\kappa}x) & \text{for} \quad \kappa < 0. \end{cases} \tag{4}$$

The second class of considered Hamiltonia systems is defined by

$$H = \frac{1}{2}\left(p_r^2 + \frac{p_\varphi^2}{\mathrm{S}_\kappa(r)^2}\right) + V(r,\varphi), \qquad V(r,\varphi) = \mathrm{S}_\kappa^k(r)U(\varphi), \tag{5}$$

where $k \in \mathbb{Z}$ and $U(\varphi)$ is a meromorphic function of variable φ, for details see [3]. This is a natural Hamiltonian system defined on $T^\star M^2$ for the prescribed M^2. Notice that the kinetic energy as well as the potential depends of the curvature κ.

It appears that for both these classes of Hamiltonian systems we can find certain particular solutions and we are able to perform successfully differential Galois integrability analysis. As result we obtain that necessary conditions for the integrability put obstructions on admissible values of the following function

$$\lambda := 1 + \frac{U''(\varphi_0)}{kU(\varphi_0)}. \tag{6}$$

where $\varphi_0 \in \mathbb{C}$ satisfies $U'(\varphi_0) = 0$ and $U(\varphi_0) \neq 0$. Some examples of applications of theses conditions and integrable systems are presented.

References

[1] Herranz F. J., Ortega R., Santander M. *Trigonometry of spacetimes: a new self-dual approach to a curvature/signature (in)dependent trigonometry*// *J. Phys. A: Math. Gen.*, vol. 33, 4525–4551.

[2] Maciejewski A. J., Przybylska. *Darboux points and integrability of Hamiltonian systems with homogeneous polynomial potential*// *J. Math. Phys.*, 2005, vol. 46, no. 6, 062901, 33 pp.

[3] Maciejewski A. J., Szumiński W., Przybylska M. *Note on integrability of certain homogeneous Hamiltonian systems in 2D constant curvature spaces*// Phys. Lett. A, submitted.

[4] Szumiński W., Maciejewski A. J., Przybylska M. *Note on integrability of certain homogeneous Hamiltonian systems*// Phys. Lett. A, 2015, vol. 379, no. 45–46, pp. 2970–2976.

[5] Morales Ruiz J. J. *Differential Galois theory and non-integrability of Hamiltonian systems.* Birkhäuser Verlag, Basel, 1999.

[6] Przybylska M., *Darboux points and integrability of homogenous Hamiltonian systems with three and more degrees of freedom*// *Regul. Chaotic Dyn.*, 2009, vol. 14, np. 2, 263–311.

On the stability of two-link trajectory of the parabolic Birkhoff billiards

Anatoly P. Markeev

A. Ishlinsky Institite for Problems in Mechanics, Russian Academy of Sciences, Moscow, Russia

We study the inertial motion of a material point in a planar domain bounded by two coaxial parabolas. Inside the domain the point moves along a straight line, the collision with the boundary curves are assumed to be perfectly elastic. There is a two-link periodic trajectory, for which the point alternately collides with the boundary parabolas at their vertices, and in the intervals between collisions it moves along the common axis of the parabolas. We study the nonlinear problem of stability of the two-link trajectory of the point.

This research was supported by the Russian Foundation for Basic Research (14.01.00380).

Tracking of lines in spherical images via sub-Riemannian geodesics on $SO(3)$

Alexey Mashtakov[1], R. Duits[2], Yu. Sachkov[1], E. Bekkers[2] and I. Beschastnyi[3]

[1] *Program Systems Institute of RAS, Pereslavl-Zalesskiy, Russia*
[2] *Eindhoven University of Technology, Eindhoven, Netherlands*
[3] *International School for Advanced Studies, Trieste, Italy*

In some imaging applications (e.g. in retinal imaging) it is natural to model the data by spherical images. In previous work [3] we proposed a framework for tracking of lines in flat images via sub-Riemannian geodesics on Lie group $SE(2)$. Here we extend the framework for tracking of lines in *spherical* images. This requires a sub-Riemannian manifold structure in a different Lie group, namely the group $SO(3)$ (consisting of 3D-rotations) acting transitively on the 2-sphere S^2.

In order to detect salient lines in these images we consider the problem of minimizing the functional $\int_0^l C(\gamma(s))\sqrt{\xi^2 + k_g^2(s)}\,\mathrm{d}s$ for a curve γ on a sphere with fixed boundary points and directions. The total length l is free, s denotes the spherical arclength, and k_g denotes the geodesic curvature of γ. Here the analytic external cost $C \geq \delta > 0$ is obtained from spherical data. We lift this problem to the sub-Riemannian (SR) problem on Lie group $SO(3)$, and show that the spherical projection of certain SR-geodesics provides a solution to our curve optimization problem. In fact, this holds only for the geodesics whose spherical projection does not exhibit a cusp (cf. [4]).

For $C = 1$ we derive SR-geodesics and evaluate the first cusp time. We show that these curves have a simpler expression when they are parameterized by spherical arclength rather than by sub-Riemannian arclength. The case $C \neq 1$ (data-driven SR-geodesics) we solve via a SR Fast Marching method. Finally we show an experiment of vessel tracking in a spherical image of the retina, and study the effect of including the spherical geometry in analysis of vessels curvature.

References

[1] Mashtakov A., Duits R., Sachkov Yu., Bekkers E., Beschastnyi I. *Tracking of Lines in Spherical Images via Sub-Riemannian Geodesics on* $SO(3)$// ArXiv, 1604.03800, 2016.

[2] Mashtakov A. P., Ardentov A. A., Sachkov Y. L., *Parallel Algorithm and Software for Image Inpainting via Sub-Riemannian Minimizers on the Group of Rototranslations*// Numerical Mathematics: Theory, Methods and Applications, 2013, vol. 6, no. 1, pp. 95-115.

[3] Bekkers E. J., Duits R., Mashtakov A., Sanguinetti, G. R. (joint main authors). *A PDE Approach to Data-driven Sub-Riemannian Geodesics in* $SE(2)$// SIAM Journal on Imaging Sciences, 2015, 8:4, pp. 2740-2770.

[4] Duits R., Boscain U., Rossi F., Sachkov Y. L., *Association Fields via Cuspless Sub-Riemannian Geodesics in* $SE(2)$// JMIV, 2014, 49 (2), pp. 384–417.

Relative equilibria for the 2-body problem in the hyperbolic plane

Luis C. García Naranjo[1], Juan C. Marrero[2], Ernesto Pérez-Chavela[3] and Miguel Rodríguez-Olmos

[1] *Depto. Matemáticas y Mecánica, IIMAS-UNAM, Mexico City, Mexico*
[2] *ULL-CSIC Geometría Diferencial y Mecánica Geométrica. Departamento de Matemática Fundamental, Facultad de Matemáticas, Universidad de la Laguna, La Laguna, Tenerife, Canary Islands, Spain*
[3] *Departamento de Matemáticas, Universidad Autónoma Metropolitana-Iztapalapa, Mexico City, Mexico*
[4] *Universitat Politècnica de Catalunya, Barcelona, Spain*

I will present the results of our recent paper [2] where we classify and analyze the stability of all relative equilibria for the two-body problem in the hyperbolic space of dimension 2.

Our contribution is to show that, for the 2-body problem in the hyperbolic plane, the only relative equilibria arise as conjugation of the so-called “elliptic” and “hyperbolic” relative equilibria found before in [1]. Moreover, we show that all of the hyperbolic relative equilibria are unstable and establish necessary and sufficient conditions for nonlinear stability of the elliptic relative equilibria. Such conditions are given in terms of the ratio of the masses and the hyperbolic distance between the particles. All of our results are formulated in terms of the intrinsic Riemannian data of the problem so they are valid in any model of the hyperbolic plane.

References

[1] Diacu, F., Pérez-Chavela, E., Reyes, J.G., An intrinsic approach in the curved n–body problem. The negative case. *Journal of Differential Equations*, **252**, 4529–4562, (2012).

[2] García Naranjo L.C., Marrero J.C., Pérez-Chavela E., Rodríguez-Olmos M., Classification and stability of relative equilibria for the two-body problem in the hyperbolic space of dimension 2, *Journal of Differential Equations*, **260**, 6375–6404, (2016).

The dynamics of an articulated n-trailer vehicle

Alejandro Bravo-Doddoli[1] and Luis C. García Naranjo[2]

[1] *Depto. de Matemáticas, Facultad de Ciencias, UNAM, Circuito Exterior S/N, Ciudad Universitaria, Mexico City, Mexico*
[2] *Depto. Matemáticas y Mecánica, IIMAS-UNAM, Mexico City, Mexico*

We derive the reduced equations of motion for an articulated n-trailer vehicle that moves under its own inertia on the plane. We show that the energy level surfaces in the reduced space are $(n+1)$-tori and we classify the equilibria within them, determining their stability. A thorough description of the dynamics is given in the case $n = 1$. The main results of this work were recently published in [1].

References

[1] Bravo-Doddoli A. and García Naranjo L.C., The dynamics of an articulated n-trailer vehicle, *Regular and Chaotic Dynamics*, **20**, 497–517, (2015).

Transient and periodic spatiotemporal structures in a reaction-diffusion-mechanics system

Grigory V. Osipov[1], V.A. Kostin[1,2]

[1] *National Research University Higher School of Economics, Nizhny Novgorod, Russia*
[2] *Institute of Applied Physics, Russian Academy of Sciences, Nizhny Novgorod, Russia*

The reaction-diffusion-mechanics models are the models used to describe self-consistent electromechanical activity in a cardiac muscle. Such models couples two mechanisms of signal spreading in the tissue: the slow (reaction-diffusion) spreading of electrical excitation and the fast (almost instantaneous) spreading of mechanical deformations. This coupling may significantly modify the electrical excitation spreading and corresponding contractile activity with emergence of new spatiotemporal structures and patterns, which modification is not yet completely understood even in the one-dimensional case of a single muscle fiber. We propose clear convenient model which allows one to study the electromechanical activity of such a fiber in relation to the mechanical parameters of fiber fixation (such as stiffness of tissue fixation and the applied mechanical load, which can be easily controlled in experiments). Using this model, we determine and analyze the physical origin of the primary dynamical effects which can be caused by electromechanical coupling and mechanoelectrical feedback in a cardiac tissue.

On the basis of the reaction-diffusion-mechanics model with the self-consistent electromechanical coupling, we have numerically analyzed the emergence of structures and wave propagation in the excitable contractile fiber for various contraction types (isotonic, isometric, and auxotonic) and electromechanical coupling strengths. We have identified two main regimes of excitation spreading along the fiber: (i) the common quasi-steady-state propagation and (ii) the simultaneous ignition of the major fiber part and have obtained the analytical estimate for the boundary between the regimes in the parameter space. The uncommon oscillatory regimes have been found for the FitzHugh—Nagumo-like system: (i) the propagation of the soliton-like waves with the boundary reflections and (ii) the clusterized self-oscillations. The single space-time localized stimulus has been shown to be able to induce long-lasting transient activity as a result of the after-excitation effect when the just excited fiber parts are reexcited due to the electromechanical global coupling. The results obtained demonstrate the wide variety of possible dynamical regimes in the electromechanical activity of the cardiac tissue and the significant role of the mechanical fixation properties (particularly, the contraction type), which role should be taken into consideration in similar studies. In experiments with isolated cardiac fibers and cells, these parameters can be relatively easily controlled, which opens a way to assess electrical and mechanical parameters of the fibers and cells through analysis of dynamical regimes as dependent on fixation stiffness and external force. In real heart, high blood pressure and hindered blood flow play similar role to the applied external force and increased fixation stiffness. Our results provide a hint of how such global (i.e., associated with the large areas of the heart tissue) parameters can affect the heart electrical and contraction activity.

Elliptical billiards with Hooke's potential

Milena Radnovic

Mathematical Institute of the Serbian Academy of Sciences and Arts, Beograd, Serbia

We present a topological description of elliptical billiards with the Hooke's potential, using Fomenko invariants.

Optimal synthesis for the left-invariant sub-Riemannian problem on the group of hyperbolic motions of the plane

Yuri L. Sachkov[1] and Yasir Awais Butt[2]

[1] *Program Systems Institute, Pereslavl-Zalessky, Russia*
[2] *Muhammad Ali Jinnah University, Islamabad, Pakistan*

We consider the left-invariant sub-Riemannian structure on the group $\mathrm{SH}(2)$ of hyperbolic motions of the plane. Sub-Riemannian minimizers are solutions to the optimal control problem

$$\begin{aligned}
&\dot{x} = u_1 \cosh z, \quad \dot{y} = u_1 \sinh z, \quad \dot{z} = u_2,\\
&q = (x, y, z) \in \mathbb{R}^3, \quad (u_1, u_2) \in \mathbb{R}^2,\\
&q(0) = q_0, \qquad q(t_1) = q_1,\\
&\int_0^{t_1} \sqrt{u_1^2 + u_2^2} \to \min .
\end{aligned}$$

Sub-Riemannian geodesics are parameterized by Jacobian elliptic functions. The group of symmetries of the problem are described. Local and global optimality of geodesics is characterized. The cut locus (set of points where geodesics lose optimality) is globally described. A complete optimal synthesis is constructed.

References

[1] Butt Y. A., Sachkov Yu. L., Bhatti A. I. *Extremal trajectories and Maxwell strata in sub-Riemannian problem on group of motions of pseudo-Euclidean plane*// Journal of Dynamical and Control Systems, 20(3):341–364, July 2014.

[2] Butt Y. A., Sachkov Yu. L., Bhatti A. I. *Maxwell strata and conjugate points in the sub-Riemannian problem on the Lie group SH(2)*// Journal of Dynamical and Control Systems, accepted

[3] Butt Y. A., Sachkov Yu. L., Bhatti A. I. *Cut locus and optimal synthesis in sub-Riemannian problem on the Lie group SH(2)*, submitted.

Routes to chaos in the nonholonomic model of Chaplygin top

Igor R. Sataev[1] and Alexey O. Kazakov[2,3]

[1] *Kotel'nikov's Institute of Radio-Engineering and Electronics of RAS, Saratov Branch, Saratov, Russia*
[2] *National Research University Higher School of Economics, Nizhny Novgorod, Russia*
[3] *Udmurt State University, University, Izhevsk, Russia*

We consider the motion of a dynamically asymmetrical ball on a plane in the gravity field. The center of mass of the ball does not lie on any planes of inertia, and the point of contact of the ball with the plane is subject to a nonholonomic constraint which forbids slipping. Following [1] we call such a ball Chaplygin top.

The aim of this study is to investigate the typical scenarios of the appearance and evolution of strange attractors in the nonholonomic model of Chaplygin top. Our interest in nonholonomic models is caused by the fact that (as was shown in previous studies [2, 3]) such systems exhibit a wide variety of new interesting examples of strange attractors that are typical for the three-dimensional maps [4]. For example, our recent research [5] shows that the nonholonomic model of Chaplygin top demonstrates the so called “figure-eight” strange attractor, which relates to pseudohyperbolic strange attractors [4].

Here we show that the nonholonomic model of Chaplygin top demonstrates a comprehensive variety of scenarios of torus attractors breakup, in particular, in accordance with the mechanism of Afraimovich-Shilnikov [6], including Feigenbaum cascade inside the synchronization domain, and via torus doubling cascade [7]. In addition, the model exhibits some typical sequences of bifurcations of regular and chaotic attractors, which include the above basic scenarios of tori destruction as their stages. One of such metascenarios results in a discrete heteroclinic Shilnikov attractor [4], Fig. 1.

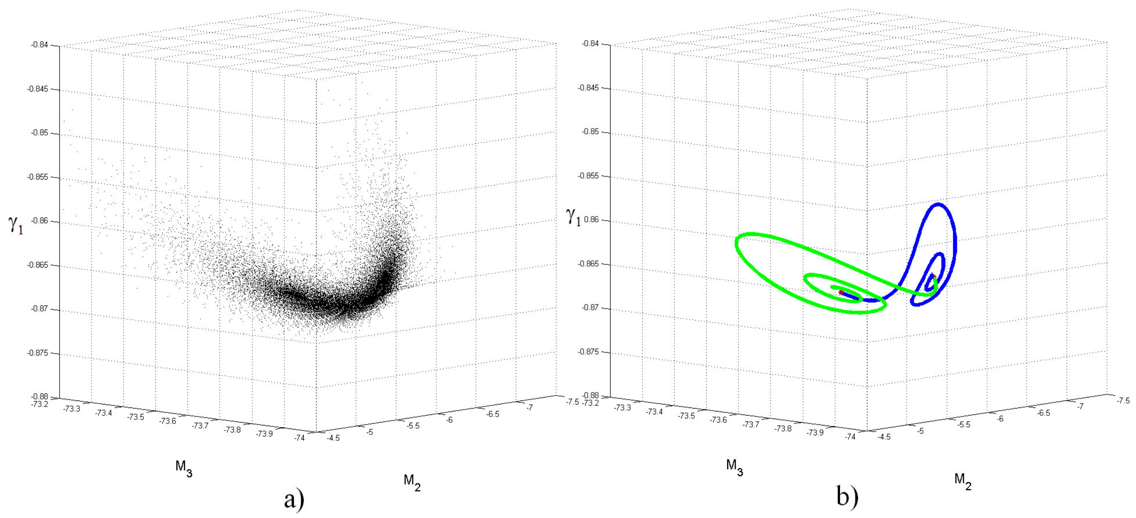

Fig. 1. a) Discrete heteroclinic Shilnikov attractor; b) heteroclinic cycle.

Another feature of the dynamics of nonholonomic model of Chaplygin top is the presence of a developed multistability. Evolution of coexisting attractors may here proceed in accordance with the scenario, which results in a strange attractor, that coincides with the homo-(hetero-)clinical structure of saddle limit cycle, which lies on the border of the basins of attraction of initially coexisting attractors. One such scenario was found to occur in the model under investigation. It results in the chaotic ring heteroclinic attractor, Fig. 2.

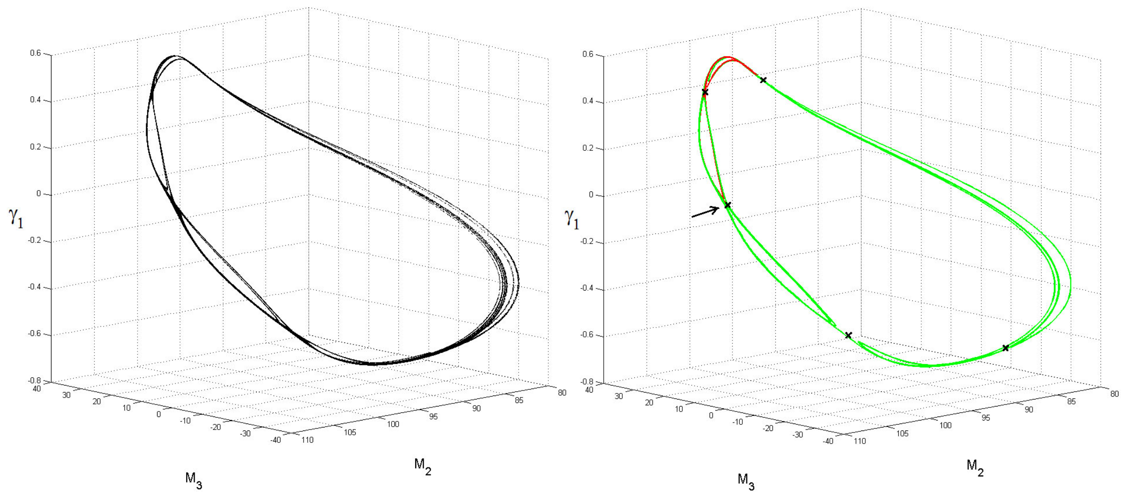

Fig. 2. a) Ring heteroclinic attractor; b) unstable invariant manifolds of the saddle cycle.

This work was supported by RSF grant No 15-12-20035.

References

[1] Shen J., Schneider D. A., Bloch A. M. *Controllability and motion planning of a multibody Chaplygin's sphere and Chaplygin's top*// Int. J. Robust Nonlinear Control, 2008, vol. 18, no. 9, pp. 905-945.

[2] Borisov A. V., Jalnine A. Y., Kuznetsov S. P., Sataev I. R., Sedova, J. V. Dynamical phenomena occurring due to phase volume compression in nonholonomic model of the rattleback // Regular and Chaotic Dynamics. 2012. vol. 17. No. 6. pp. 512-532.

[3] Gonchenko A. S., Gonchenko S. V., Kazakov A. O. Richness of chaotic dynamics in nonholonomic models of a Celtic stone // Regular and Chaotic Dynamics. 2013. vol. 18. no. 5. pp. 521-538.

[4] Gonchenko A., Gonchenko S., Kazakov A., Turaev D. *Simple Scenarios of Onset of Chaos in Three-Dimensional Maps*// International Journal of Bifurcation and Chaos. 2014. vol. 24. no. 08.

[5] Borisov A. V., Kazakov A. O., Sataev I. R. *The Reversal and Chaotic Attractor in the Nonholonomic Model of Chaplygin's Top*// Regular and Chaotic Dynamics, 2014, vol. 19, no 6, 718-733.

[6] Afraimovich V. S., Shilnikov L. P. *Invariant Two-Dimensional Tori, Their Breakdown and Stochasticity*// Methods of qualitative theory of differential equations. University Gorky. 1983. pp. 3-25.

[7] Arneodo A., Coullet P. H., Spiegel E. A. *Cascade of period doublings of tori*// Physics Letters A. 1983. vol. 94. no. 1. pp. 1-6.

Whitney smooth families of invariant tori in the reversible context 2 of KAM theory

Mikhail B. Sevryuk

V. L. Talroze Institute of Energy Problems of Chemical Physics (RAS), Moscow, Russia

In an overwhelming majority of the works on the reversible KAM theory, the reversing involution has the form

$$G_1 : (x, y, z) \mapsto (-x, y, Kz),$$

where $x \in \mathrm{T}^n = (\mathrm{R}/2\pi\mathrm{Z})^n$, y ranges in a domain $D \subset \mathrm{R}^m$, z ranges in a neighborhood of the origin of R^{2p}, K is an involutive $2p \times 2p$ matrix with eigenvalues 1 and -1 of multiplicity p each, and one is looking for invariant n-tori close to the tori $\{y = \mathrm{const},\ z = 0\}$. In this case, the dimension of the fixed point manifold of the reversing involution ($m + p$) is *no less* than half the phase space codimension of the invariant tori ($m + 2p$), and such a setup is called the *reversible context 1*.

However, nothing prevents one from considering systems reversible with respect to the involution

$$G_2 : (x, y, z) \mapsto (-x, -y, Kz),$$

where now y ranges in a neighborhood of the origin of R^m ($m \geq 1$) and the problem is to construct an invariant n-torus close to the torus $\{y = 0,\ z = 0\}$. Here the dimension of the fixed point manifold of the reversing involution (p) is *smaller* than half the phase space codimension of the invariant torus ($m + 2p$), and such a setting is referred to as the *reversible context 2*. Since the G_2-reversible system $\dot{x} = \omega$, $\dot{y} = a$, $\dot{z} = 0$ admits no invariant tori however small $a \neq 0$ is (the reversibility with respect to G_2 does not preclude a drift along the variable y), the reversible context 2 requires the presence of many external parameters (at least $m + 1$).

Some preliminary results pertaining to the reversible KAM theory in context 2 were obtained in our papers [1, 2, 3]. In these works, one deals with analytic families of analytic reversible systems, the main technical tool is Moser's modifying terms theory [4], and Cantor families of analytic invariant tori in the product of the phase space and the parameter space are constructed. According to the general principles of KAM theory, such families of invariant tori are expected to be smooth in the sense of Whitney, but this was not proven in [1, 2, 3] (the techniques of [4] are rather limited).

Our new result is as follows. Consider an $(n+m+s)$-parameter analytic family of G_2-reversible analytic systems

$$\begin{aligned} \dot{x} &= \omega + \xi(y, z, \omega, \sigma, \mu) + f(x, y, z, \omega, \sigma, \mu), \\ \dot{y} &= \sigma + \eta(y, z, \omega, \sigma, \mu) + g(x, y, z, \omega, \sigma, \mu), \\ \dot{z} &= Q(\omega, \mu)z + \zeta(y, z, \omega, \sigma, \mu) + h(x, y, z, \omega, \sigma, \mu). \end{aligned} \tag{1}$$

Here $\omega \in \mathrm{R}^n$, $\sigma \in \mathrm{R}^m$, and $\mu \in \mathrm{R}^s$ are external parameters (ω ranges in a neighborhood of some point $\omega_* \in \mathrm{R}^n$ while σ and μ range in neighborhoods of the origins of R^m and R^s, respectively), Q is a $2p \times 2p$ matrix-valued function satisfying the identity $KQ(\omega, \mu) \equiv -Q(\omega, \mu)K$,

$$\xi = O(|y| + |z|), \quad \eta = O(|y|^2 + |z|^2), \quad \zeta = O(|y|^2 + |z|^2 + |\sigma|^2),$$

and the functions f, g, h are small perturbation terms. It is also assumed that $\det Q(\omega_*, 0) \neq 0$ and that the mapping $\mu \mapsto Q(\omega_*, \mu)$ is a *versal unfolding* of the matrix $Q(\omega_*, 0)$ in the space of $2p \times 2p$ matrices anti-commuting with K (with respect to the adjoint action of the group of non-singular $2p \times 2p$ matrices commuting with K) [5]. This implies that any $2p \times 2p$ matrix anti-commuting with K and sufficiently close to $Q(\omega_*, 0)$ is equal to $AQ(\omega_*, \mu)A^{-1}$ for a suitable μ close to 0 and a suitable $2p \times 2p$ matrix A commuting with K and close to the identity matrix.

Then, roughly speaking, the following holds. For *any* values ω_0, μ_0 of the external parameters ω, μ such that the pair $(\omega_0,\ Q(\omega_0, \mu_0))$ satisfies a certain Diophantine condition, there are values ω', σ', μ' (close to ω_0, 0, μ_0, respectively) of the external parameters ω, σ, μ such that the system (1) at

$$\omega = \omega', \quad \sigma = \sigma', \quad \mu = \mu' \tag{2}$$

after a nearly identical analytic change of variables $(x, y, z) \longmapsto (x', y', z')$ commuting with G_2 takes the form

$$\dot{x}' = \omega_0 + O(|y'| + |z'|), \quad \dot{y}' = O(|y'|^2 + |z'|^2), \quad \dot{z}' = Q(\omega_0, \mu_0)z' + O(|y'|^2 + |z'|^2)$$

(provided that f, g, h are small enough). Moreover, the values ω', σ', μ' and the coordinate change $(x, y, z) \longmapsto (x', y', z')$ depend on ω_0, μ_0 in a Whitney C^∞ way.

In other words, whenever the pair $(\omega_0,\ Q(\omega_0, \mu_0))$ meets a suitable Diophantine condition, the perturbed system (1) at the *shifted* parameter values (2) possesses an invariant analytic n-torus $\{y' = 0,\ z' = 0\}$ with the *same* frequency vector ω_0 and the *same* normal behavior (characterized by the matrix $Q(\omega_0, \mu_0)$) as the unperturbed invariant n-torus $\{y = 0,\ z = 0\}$ at the parameter values

$$\omega = \omega_0, \quad \sigma = 0, \quad \mu = \mu_0.$$

All the perturbed invariant n-tori constitute a Whitney C^∞ family.

We prove this theorem by reducing it to a special case of the so-called BCHV theorem [6] concerning the reversible context 1 with singular normal behavior of invariant tori. To carry out such a reduction, one treats σ as an additional phase space variable (satisfying the equation $\dot{\sigma} = 0$) and then replaces the equation $\dot{\sigma} = 0$ by the equation $\dot{\sigma} = \Lambda y$ where Λ is a new additional external parameter ranging in a neighborhood of the origin of the space of $m \times m$ matrices. The reversing involution of the augmented phase space is $\mathcal{G} : (x, y, \sigma, z) \mapsto (-x, -y, \sigma, Kz)$. The main step in the proof is to verify that a shift along the parameter Λ vanishes.

The author is grateful to H. Hanßmann for fruitful discussions on the paper [6].

References

[1] Sevryuk M. B. *The reversible context 2 in KAM theory: the first steps* // Regul. Chaotic Dyn., 2011, vol. 16, nos. 1–2, pp. 24–38.

[2] Sevryuk M. B. *KAM theory for lower dimensional tori within the reversible context 2* // Mosc. Math. J., 2012, vol. 12, no. 2, pp. 435–455.

[3] Sevryuk M. B. *Quasi-periodic perturbations within the reversible context 2 in KAM theory* // Indag. Math. (N. S.), 2012, vol. 23, no. 3, pp. 137–150.

[4] Moser J. *Convergent series expansions for quasi-periodic motions* // Math. Ann., 1967, vol. 169, no. 1, pp. 136–176.

[5] Sevryuk M. B. *Reversible linear systems and their versal deformations* // J. Soviet Math., 1992, vol. 60, no. 5, pp. 1663–1680.

[6] Broer H. W., Ciocci M. C., Hanßmann H., Vanderbauwhede A. *Quasi-periodic stability of normally resonant tori* // Phys. D, 2009, vol. 238, no. 3, pp. 309–318.

Classical Hamiltonian systems, Lagrangian manifolds and Maslov indices, corresponding to spectra of Schroedinger operators with delta-potentials

Andrei Shafarevich

Moscow State University, Moscow, Russia

We study spectral series of the Schroedinger operator with delta-type potential on 2D or 3D Riemannian spherically symmetric manifold. Lagrangian manifolds, corresponding to these series, do not coincide with the standard Liouville tori. We describe topological structure of these manifolds as well as Maslov indices, entering quantization conditions. In particular, we study the effect of the jump of the Maslov index via passing through the critical values of the multipliers of the delta-functions.

Bifurcation analysis of a 2D rigid circular cylinder interacting dynamically with a point vortex in the absence of circulation

Sergey V. Sokolov[1], Sergey M. Ramodanov[2] and Pavel E. Ryabov[1,3]

[1] *Institute for Machines Science RAS, Moscow, Russia*
[2] *Institute for Cryptosystems, Communications and Informatics, Moscow, Russia*
[3] *Financial University under Government of the Russian Federation, Moscow, Russia*

We consider the dynamics of a system that consists of a circular cylinder interacting with a vortex filament parallel to the cylinder's element in an unbounded volume of ideal fluid. The fluid is assumed to be incompressible and at rest at infinity. The governing equations were first obtained in [1], while the Hamiltonian form of the equations and their Liouville integrability was established in [2]. In the gravity field this system was studied in [3] where it was shown to exhibit chaotical behavior and therefore be no longer integrable.

The paper [4] addresses the topology of the integrable system (a cylinder plus a single vortex). The fluid's circulation about the cylinder was assumed to be different from zero. However, it was specially noted that the case of zero circulation needs a thorough separate treatment.

Thus, this contribution is devoted to the case of zero circulation. We have obtained new intriguing invariant relations, built up the bifurcation diagram and explored bifurcations of the Liouville tori.

The work is supported by the grants of RFBR Nos. 16-01-00170 and 16-01-00809.

References

[1] Ramodanov S. M. *Motion of a circular cylinder and a vortex in an ideal fluid*. Regular and Chaotic Dynamics, 2001, vol. 6, no. 1, pp. 33–38.

[2] Borisov A. V., Mamaev I. S. *Integrability of the Problem of the Motion of a Cylinder and a Vortex in an Ideal Fluid* // Math. Notes, 2004, vol. 75, no. 1, pp. 19–22.

[3] Sokolov S. V., Ramodanov S. M. *Falling motion of a circular cylinder interacting dynamically with a point vortex* // Regular and Chaotic Dynamics, 2013, vol. 18, nos. 1-2, pp. 184–193

[4] Borisov A. V., Ryabov P. E., Sokolov S. V. *Bifurcation analysis of the Problem of Motion of a Cylinder and a Vortex in an Ideal Fluid* // Math. Notes, 2016, vol. 99, no. 6, pp. 848–854

Nontrivial analogy of finite-core and point vortices in a two-layer rotating fluid

Mikhail A. Sokolovskiy[1,2]

[1] *Water Problems Institute of RAS, Moscow, Russia*
[2] *P.P. Shirshov Institute of Oceanology of RAS, Moscow, Russia*

It is known that the theory of point vortices adequately describes the trajectory behaviors of the distributed eddy centers, if these centers are spaced far enough. However, there is a deeper connection between discrete and continuous approaches. Let us demonstrate this with the example of the family of two-layer compensated geostrophic vortices.

The analysis of stability with respect to small perturbations of circular contours of unit-radius vortex patches which compose a two-layer vortex with zero total potential vorticity (a heton) has shown [1] that this vortex is neutrally stable only if $\gamma < 1.705$. Here $\gamma = R/R_d$, where R is the characteristic horizontal scale, and R_d is the so-called Rossby radius of deformation [2]. Figure 1a shows the curves of neutral stability modes with m belonging to the plane of the parameters (h_1, γ) (h_1 is the nondimensional depth of upper layer), so that area of the mode with the corresponding number is located above each curve $h_1 = 0.5\left[1 \pm \sqrt{\Big(1/2m - L_1(\gamma)\Big)\Big(1/2m - L_m(\gamma)\Big)}\right]$. Here $L_m(\gamma) = K_m(\gamma)I_m(\gamma)$ is the product of Modified Bessel functions of mth order.

We found that there is a direct analogy between the instability criterion of m-th mode of the distributed circular heton and the transition condition for a system composed of m uniformly distributed discrete hetons located along the circles of both layers for beginning the infinite type of motion in the form of m two-layer vortex pairs radially running away.

We can note that:

- If γ is greater then its critical value γ_{cr}^m, then the originally vertical m discrete heton axes tilt, and the newly formed two-layer pairs will move away along radial directions. The finite-core dipole structures that form as the result of collapse of an unstable finite-size heton behave in a similar manner.

- The asymptotics $\gamma_{cr}^m \sim m$, which implies a linear dependence between the critical values of stratification parameter γ_m and the numbers of high unstable modes m, is still valid in discrete case up to proportionality factor $(\gamma_{cr}^m)_{discr} \sim \alpha m$, $\alpha \approx 0.37$.

  However, one should take into account the fundamental difference between the two models: for discrete vortices at $\gamma > (\gamma_{cr}^m)_{discr}$, a system of m radially scattering pairs always form, while for a finite-core heton, the value of γ_{cr}^m determines only the lower boundary of the domain in which the mode with number m becomes unstable, and the conditions of realization of this mode are not necessarily preferable.

- Nevertheless, this analogy enables a mathematical explanation to be given for the possible separation mechanism of distributed pairs: **for a newly formed vortex pair to start moving away from the center of the original vortex, it is necessary that its local vorticity center fall beyond the separatrix bounding the domain of finite motions of the appropriate system of discrete vortexes**.

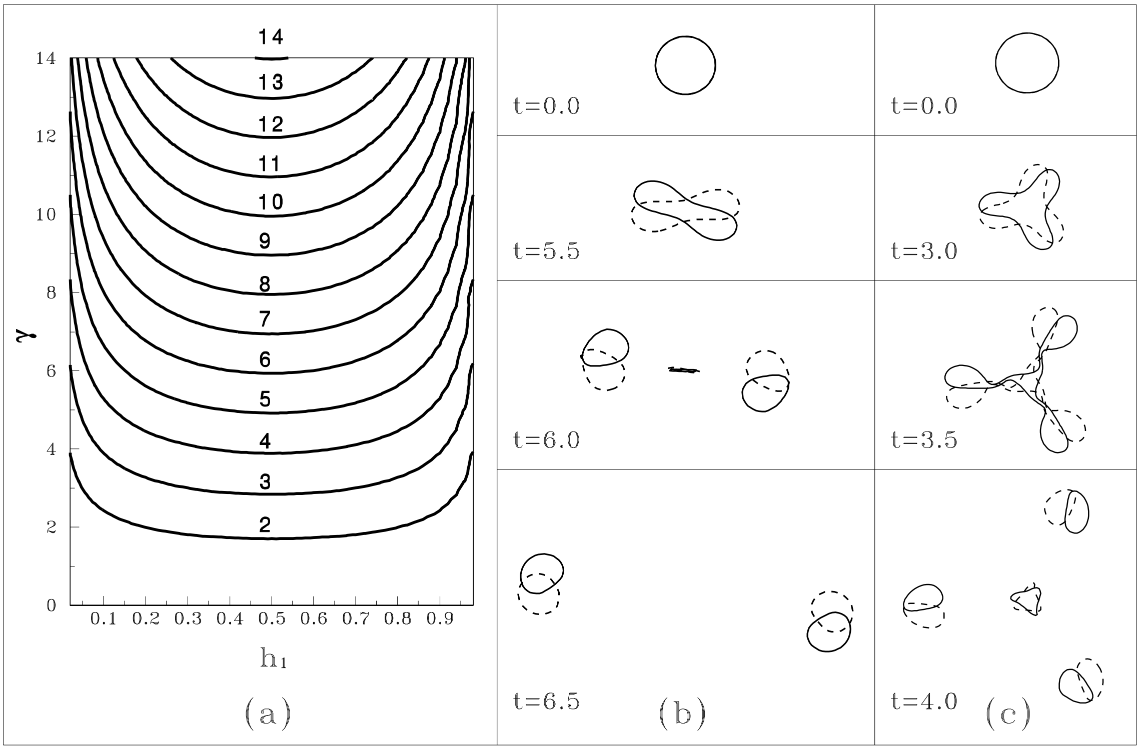

Fig. 1. (a) Heton neutral-stability curve on the plane of parameters ($h_1,\ \gamma$) of modes with indicated numbers. Configurations of contours of the top (full lines) and bottom (dashed lines) layers for an unstable heton at $h_1 = 0.5$ in the specified moments of dimensionless time: (b) $\gamma = 2.4$; (c) $\gamma = 4$.

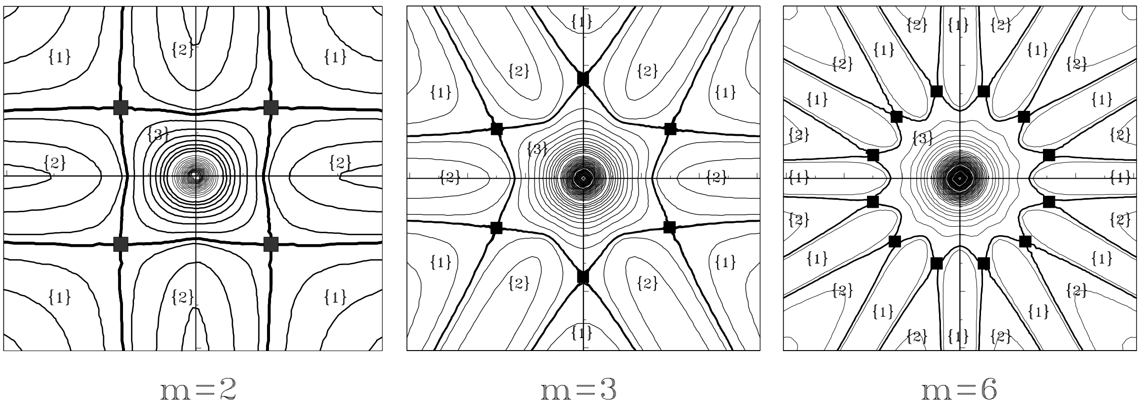

Fig. 2. Phase portraits, i. e. isolines of Hamiltonian of system of m vortices, uniformly distributed on circumferences with the same radius in each layer: $m = 2, 3$, $\gamma = 1$; $m = 6$, $\gamma = 2$. The denotations $\{1\}$, $\{2\}$, and $\{3\}$ refer to different types of motion. Square markers show the intersection points of separatrices.

References

[1] Kozlov, V.F., Makarov, V.G., Sokolovskiy, M.A. Numerical model of the baroclinic instability of axially symmetric eddies in two-layer ocean. *Izvestiya, Atmos. Ocean. Phys.*, 1986, vol. 22, no. 8, pp. 674–678.

[2] Sokolovskiy, M.A., Verron, J. *Dynamics of Vortex Structures in a Stratified Rotating Fluid.* Series Atmospheric and Oceanographic Sciences Library. Vol. 47, Springer: Cham - Heidelberg - New York - Dordrecht - London, 2014, 382 pp.

Motion planning and tracking control for a spherical rolling robot actuated by pendulum

Mikhail Svinin[1], Yang Bai[1], and Motoji Yamamoto[1]

[1] *Kyushu University, Fukuoka, Japan*

This paper deals with motion planning for a spherical rolling robot driven by a pendulum mounted at the center of the spherical shell. A similar problem was considered in [1]. Here in this paper, it is assumed that the pendulum is actuated by two motors. The full mathematical model of the robot combines five kinematic equations, describing the evolution of the center of the robot and its orientation, and the dynamic equations. The latter combines three differential equations for the angular acceleration of the sphere and four differential equations describing the dynamics of the pendulum. The total model contains twelve state space equations with two inputs.

It is shown that, contrary to the rolling robots actuated by symmetrical internal rotors[2, 3], the motion planning problem can be decoupled and solved separately at the levels of kinematics and dynamics. In particular, when the kinematic reference trajectory is produced by planning a pure rolling (no spinning) motion, the dynamic equations can be reduced under imposition of virtual constraints restricting the motion of the pendulum to the vertical plane tangent to the contact path in the contact plane. The reduced dynamic system, which we call the hoop-pendulum system, has just two differential equations of the second order, with the generalized coordinates given by the contact point on the reference contact curve in the plane and the pendulum angle in the vertical plane tangent to the path. The hoop-pendulum system is underactuated as there is only one control input—the projection of the control moments onto the vertical plane tangent to the path.

The controllability of the hoop-pendulum system is established and two algorithms for planning rest-to-rest movements, are proposed. One is based on the optimal control, minimizing the control effort, and another one is based on the parameterization of the pendulum angle by the second derivative of the Beta function. The feasibility of the the resulting timing control laws is verified under simulation for tracing different contact curves (straight lines, circles, generalized Viviani's curve and the Loxodrome).

Finally, a backstepping-based feedback tracking controller for the whole configuration of the spherical robot, comprising both the position and orientation, is proposed. The feasibility for the backstepping controller is first tested for the hoop-pendulum system, followed by the construction of a tracking controller for the full mathematical model. The validity of the proposed tracking controller is demonstrated by establishing the asymptotic stability of the error dynamics. The performance of the controller is verified under simulations for tracking linear and circular motions respectively.

References

[1] Ivanova T., Pivovarova E., *"Dynamics and control of a spherical robot with an axisymmetric pendulum actuator,"* *Nonlinear Dynamics & Mobile Robotics*, 2013, vol. 1, no. 1, pp. 71–85.

[2] Borisov A., Kilin A., Mamaev I., *"How to control Chaplygin's sphere using rotors. Part II,"* *Regular and Chaotic Dynamics*, 2013, vol. 18, no. 1–2, pp. 144–158.

[3] Svinin M., Morinaga A., Yamamoto M., *"On the dynamic model and motion planning for a spherical rolling robot actuated by orthogonal internal rotors,"* *Regular and Chaotic Dynamics*, 2013, vol. 18, no. 1–2, pp. 126–143.

Chaotic dynamics in the problem of free fall of a three-bladed screw in a fluid

Valentin A. Tenenev[1], Evgenii V. Vetchanin[1,2], Lenar F. Ilaletdinov[1]

[1] *Kalashnikov Izhevsk State Technical University, Izhevsk, Russia*
[2] *Udmurt State University, Izhevsk, Russia*

In this paper we consider the free fall of a homogeneous three-bladed screw consisting of a central solid sphere and blades whose shape is an oblate ellipsoid (see Fig. 1). The center of mass of the screw coincides with the center of the sphere, and thus the sum of gravity torque and buoyancy torque about the center of mass equals zero. The investigation of the motion is performed within the framework of theories of an ideal fluid and a viscous fluid.

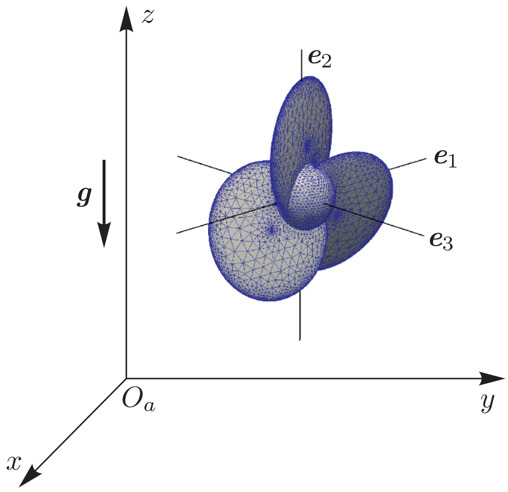

Figure 1. A three-bladed screw

To describe the motion of the body, two Cartesian coordinate systems are introduced: a fixed one, O_axyz, and a moving one, $O\boldsymbol{e}_1\boldsymbol{e}_2\boldsymbol{e}_3$, attached to the body (see Fig. 1). The origin O of the moving coordinate system coincides with the center of mass of the screw. The axis $O\boldsymbol{e}_3$ of the moving coordinate system coincides with the helical symmetry axis of the body.

The orientation of the screw blades with respect to the central sphere is determined by the angle Φ, and the plane $O\boldsymbol{e}_1\boldsymbol{e}_2$ is overlapped maximally at $\Phi = 0°$ (see Fig. 1), and this overlapping is minimal at $\Phi = 90°$.

The motion of the moving coordinate system relative to the fixed one is governed by the following kinematic relations [1]:

$$\begin{gathered}\dot{\boldsymbol{\alpha}} = \boldsymbol{\alpha} \times \boldsymbol{\Omega}, \quad \dot{\boldsymbol{\beta}} = \boldsymbol{\beta} \times \boldsymbol{\Omega}, \quad \dot{\boldsymbol{\gamma}} = \boldsymbol{\gamma} \times \boldsymbol{\Omega}, \\ \dot{x} = \boldsymbol{\alpha} \cdot \boldsymbol{V}, \quad \dot{y} = \boldsymbol{\beta} \cdot \boldsymbol{V}, \quad \dot{z} = \boldsymbol{\gamma} \cdot \boldsymbol{V},\end{gathered} \tag{1}$$

where x, y and z are the coordinates of the point O in absolute space O_axyz, $\boldsymbol{\alpha}$, $\boldsymbol{\beta}$ and $\boldsymbol{\gamma}$ are the unit vectors of the fixed coordinate system referred to the moving coordinate system, $\boldsymbol{V}$ is the velocity of the screw referred to the moving coordinate system, and $\boldsymbol{\Omega}$ is the angular velocity of the screw referred to the moving coordinate system.

The motion of the body in a resisting medium is governed by equations [2]

$$\begin{gathered}\dot{\boldsymbol{p}} = \boldsymbol{p} \times \boldsymbol{\Omega} - \mu\boldsymbol{\gamma} - \boldsymbol{F}_s, \\ \dot{\boldsymbol{M}} = \boldsymbol{M} \times \boldsymbol{\Omega} + \boldsymbol{p} \times \boldsymbol{V} - \boldsymbol{G}_s,\end{gathered} \tag{2}$$

where $\boldsymbol{p} = \mathbf{C}\boldsymbol{V} + \mathbf{B}\boldsymbol{\Omega}$ is the linear momentum, $\boldsymbol{M} = \mathbf{B}^T\boldsymbol{V} + \mathbf{A}\boldsymbol{\Omega}$ is the angular momentum, $\mathbf{C} = m\mathbf{E} + \boldsymbol{\Lambda}_1$, $\mathbf{A} = \mathbf{J} + \boldsymbol{\Lambda}_2$, m is the mass of the body, $\mathbf{J}$ is the tensor of inertia of the body, $\boldsymbol{\Lambda}_1$ is the tensor of added masses, $\boldsymbol{\Lambda}_2$ is the tensor of added moments of inertia, $\mathbf{B}$ is the tensor resulting from the helical symmetry of the body, $\mu = (\rho_b - \rho_f)Vg$ is the weigth of the body in the fluid, ρ_b is the density of the body, ρ_f is the density of the fluid, V is the volume of the body, g is the standard gravitational acceleration with $\boldsymbol{g} \uparrow\downarrow O_az$, $\boldsymbol{F}_s$ is the steady-state drag force, and $\boldsymbol{G}_s$ is the steady-state torque. The viscous drag has been described by a quadratic law, the drag coefficients have been determined using numerical simulation of the steady-state motion of the screw in a viscous fluid.

For the case of an ideal fluid ($\boldsymbol{F}_s = 0$, $\boldsymbol{G}_s = 0$), the stability of uniformly accelerated rotations is investigated. For the case of a viscous fluid, a chart of Lyapunov exponents and bifucation trees are computed. Depending on the parameters of the system, quasiperiodic and chaotic regimes of motion are possible. Examples of simple and chaotic attractors occurring in the system are shown in Fig. 2. A bifurcation tree and the dependence of Lyapunov exponents on the angle Φ are shown in Fig. 3

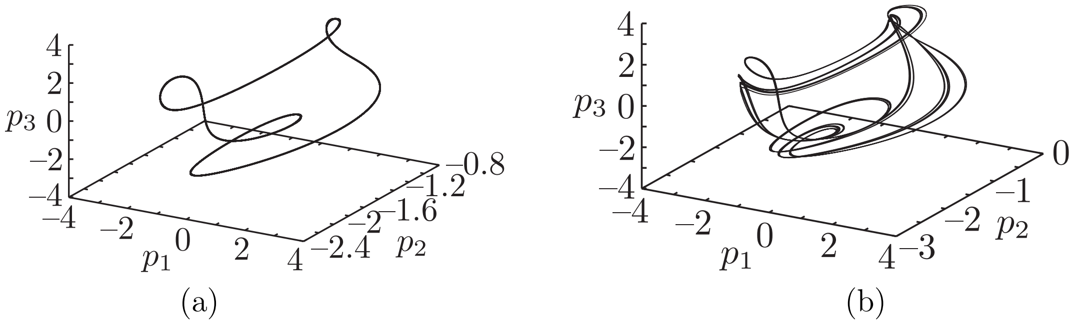

Figure 2. Projection of (a) a simple attractor and (b) a chaotic attractor onto the subspace $\{p_1p_2p_3\}$ at $\mu = 3$, $\Phi = 45.64°$.

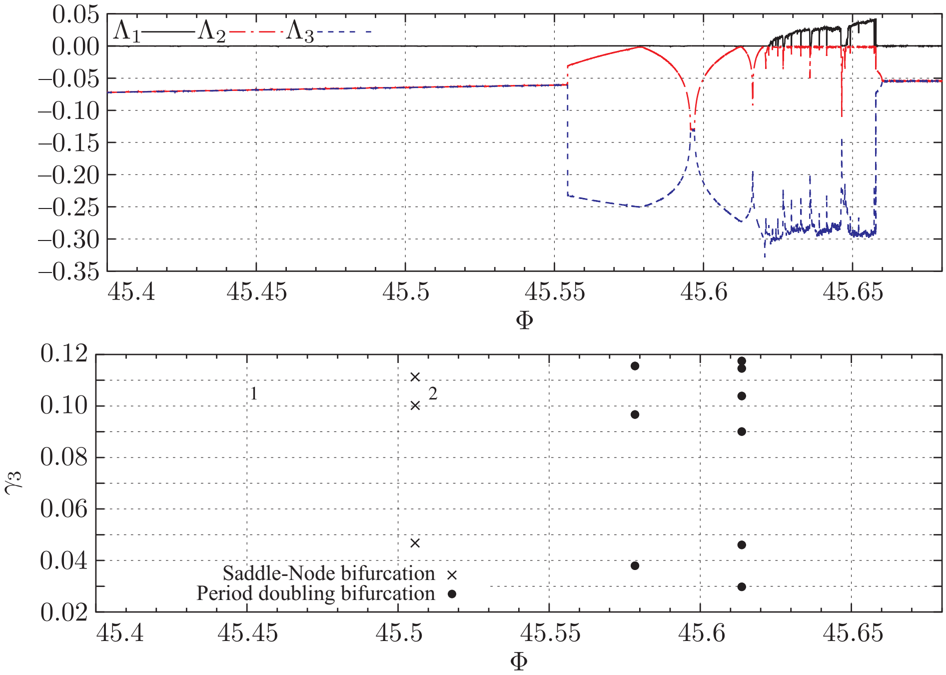

Figure 3. Bifurcation tree of the variable γ_3 at $\mu = 3$.

References

[1] Borisov A.V., Mamaev I.S. Rigid body dynamics. Hamiltonian methods, integrability, chaos, Moscow-Izhevsk: Institute of Computer Science, 2005, 576 pp.

[2] Kirchhoff G., Hensel K. Vorlesungen über mathematische Physik. Mechanik. Leipzig: BG Teubner, 1874. P.489

Abel equations and Backlund transformations

Andrey Tsyganov

St. Petersburg State University, Russia

The discretization of dynamical systems in an integrability preserving way has been widely investigated in the last decades. Potentially, it has a great impact in many different areas, such as discrete mathematics, algorithm theory, numerical analysis, statistical mechanics, etc. We show how Abel's theory incorporates discretization of the Hamilton-Jacoby equations associated with the hyperelliptic and non-hyperelliptic curves.

Dynamics of two point vortices in an external flow

Evgenii V. Vetchanin[1,2], Alexey O. Kazakov[2,3]

[1] *Kalashnikov Izhevsk State Technical University, Izhevsk, Russia*
[2] *Udmurt State University, Izhevsk, Russia*
[3] *National Research University Higher School of Economics, Nizhnii Novgorod, Russian*

In this paper we study the motion of two point vortices in an external flow consisting of two components: a shear flow [1] and a flow generated by an acoustic wave [3]. The equations of motion take the form

$$\begin{gathered}
\frac{dx_1}{dt} = -\frac{\Gamma_2}{2\pi}\frac{y_1 - y_2}{l^2}, \quad \frac{dy_1}{dt} = \frac{\Gamma_2}{2\pi}\frac{x_1 - x_2}{l^2} + \alpha x_1 + V_0 \cos\left(k y_1 - \omega t\right), \\
\frac{dx_2}{dt} = -\frac{\Gamma_1}{2\pi}\frac{y_2 - y_1}{l^2}, \quad \frac{dy_2}{dt} = \frac{\Gamma_1}{2\pi}\frac{x_2 - x_1}{l^2} + \alpha x_2 + V_0 \cos\left(k y_2 - \omega t\right), \\
l^2 = (x_1 - x_2)^2 + (y_1 - y_2)^2,
\end{gathered} \tag{1}$$

where x_i, y_i are the coordinates of the ith vortex ($i = 1, 2$), Γ_i is the intensity of the ith vortex ($i = 1, 2$), α is the vorticity of the external flow, V_0 is the amplitude of oscillation of the fluid particle velocity under the action of the acoustic wave, and k, ω are the wave number and the circular frequency of the acoustic wave. The parameters k and ω are related by $\omega = a \cdot k$, where a is the speed of sound.

Equations (1) admit only one integral of motion

$$\Gamma_1 x_1 + \Gamma_2 x_2 = P = \mathrm{const}. \tag{2}$$

By making a change of variables and rescaling time

$$\begin{gathered}
R = \frac{k}{2}\left((x_1 - x_2)^2 + (\overline{y}_1 - \overline{y}_2)^2\right)^{1/2}, \quad \varphi = \arctan\frac{\overline{y}_1 - \overline{y}_2}{x_1 - x_2}, \\
S = \frac{k}{2}(\overline{y}_1 + \overline{y}_2), \quad \tau = \omega t, \quad \overline{y}_i = y_i - at
\end{gathered}$$

and using the integral (2), the system (1) can be written in the form

$$\begin{gathered}
\dot{R} = \frac{\alpha}{2\omega}R\sin 2\varphi - \frac{V_0}{a}\sin\varphi \sin S \sin\left(R\sin\varphi\right), \\
\dot{S} = -1 + \frac{\Gamma_2 - \Gamma_1}{2\pi}\frac{\omega}{4Ra^2}\cos\varphi + \frac{\alpha}{a(\Gamma_1 + \Gamma_2)}\left(P + \frac{\Gamma_2 - \Gamma_1}{k}R\cos\varphi\right) + \frac{V_0}{a}\cos S\cos\left(R\sin\varphi\right), \\
\dot{\varphi} = \frac{(\Gamma_1 + \Gamma_2)\omega}{8\pi a^2 R^2} + \frac{\alpha}{\omega}\cos^2\varphi - \frac{V_0}{aR}\cos\varphi \sin S \sin\left(R\sin\varphi\right).
\end{gathered} \tag{3}$$

The quantity V_0/a has the meaning of the Mach number. In the air, with powerful sound waves creating pain in the ears, the Mach number is about 0.0014 [4].

We note that the classical problem of the motion of two vortices is Hamiltonian and integrable, and the equations of motion have an invariant measure. The addition of an acoustic wave makes the system nonintegrable and leads to the loss of the invariant measure, and various attracting regimes arise in the system.

An example of a Poincaré section is shown in Fig. 1a). The focus f_+^5 appears as a result of a bifurcation called *supercritical reversible pitchfork*. Fixed points f_{1+}^{10}, f_{2+}^{10}, h_1^{10}, h_2^{10} appear as a result of a *saddle-node* bifurcation. A fragment of the bifurcation diagram is shown in Fig. 1b).

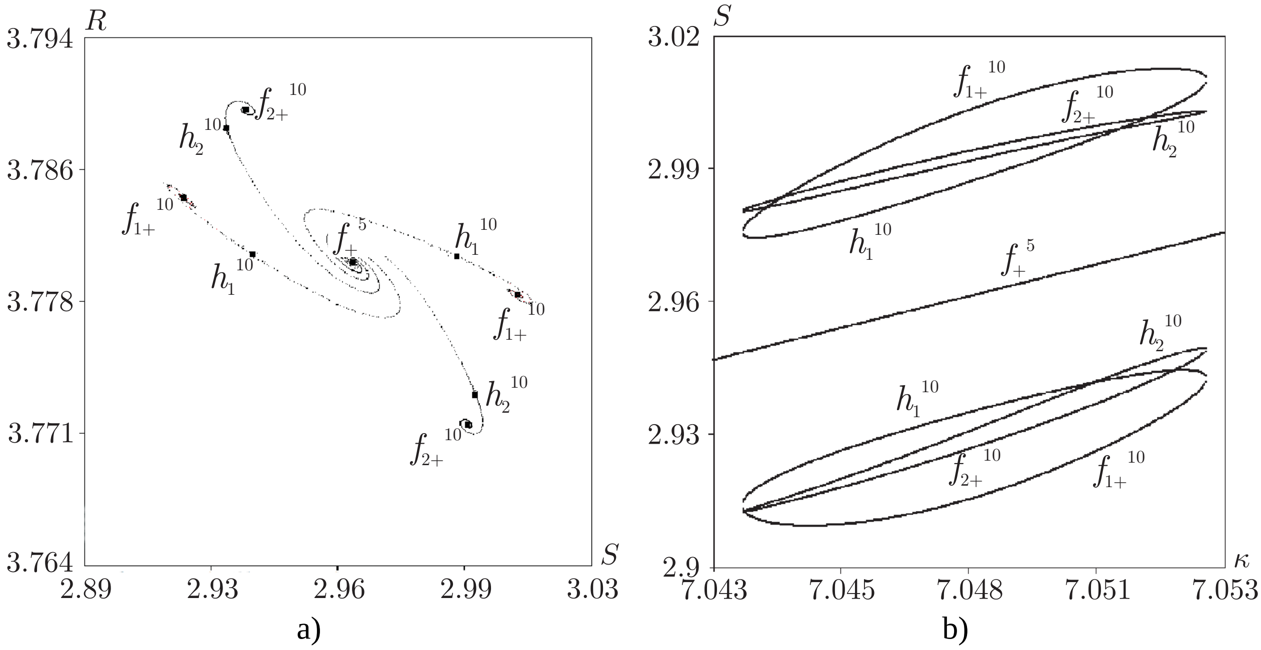

Fig. 1. (a) Poincaré section at $\alpha = 0$, $V_0/a = 0.202$, $\Gamma_1 = \Gamma_2 = \Gamma$, $\kappa = \frac{\Gamma\omega}{2\pi a^2} = 7.05$ (f_+^5 is the focus of order 5, f_{1+}^{10}, f_{2+}^{10} are the foci of order 10, and h_1^{10}, h_2^{10} are saddle points of order 10), (b) bifurcation diagram

References

[1] Bogomolov V.A. Interaction of vortices in plane-parallel flow // Izvestiya AN SSSR, vol.17, no. 2, 1981. pp. 199-201 (In Russian)

[2] Gonchar V. Y., Ostapchuk P. N., Tur A. V., Yanovsky V. V. Dynamics and stochasticity in a reversible system describing interaction of point vortices with a potential wave // Physics Letters A., 1991, vol. 152, no. 5, pp. 287-292.

[3] Vetchanin E.V., Kazakov A.O. Bifurcations and chaos in the dynamics of two point vortices in an acoustic wave, International Journal of Bifurcation and Chaos, 2016, vol. 26, no. 4, 1650063, 13 pp.

[4] Isakovich M.A. General acoustics. M.: Nauka, 1973

Uniform global asymptotic stabilization of nonlinear periodic systems by damping control

Vasiliy Zaitsev

Udmurt State University, Izhevsk, Russia

Based on the Lyapunov direct method, we get new sufficient conditions for uniform global asymptotic stabilization of nonlinear control systems with periodic coefficients by damping control. Effective sufficient conditions for asymptotic stabilization of affine and bilinear periodic systems are derived. Corollaries are obtained for bilinear periodic control system with the free dynamics defined by a linear Hamiltonian system. Examples are considered.

CONTENTS

Andrey Agrachev
Switching in time-optimal problems 4

Alain Albouy, Hildeberto Cabral
On a question by Wintner about the classification of the isosceles solutions of the 3-body problem 5

Andrey Ardentov, Yu. Sachkov and A. Pichugin
Nilpotent approximation of mobile robot with a trailer 6

Jan Awrejcewicz, Grzegorz Kudra
Bifurcation and chaos exhibited by a rattleback lying on vibrating surface modified by magnetic force 8

Boris Bardin
The special cases of degeneracy in the stability problem of an equilibrium position of a periodic Hamiltonian system 10

Eketerina Biryucheva, Sergey Sokolov, Pavel Ryabov
The integrable case of M. Adler and P.van Moerbeke - thirty years later: spectral curve, first integrals and bifurcation diagram 11

Ivan Bizyaev, Alexey Borisov, Ivan Mamaev
The dynamics of vortex sources in a deformation flow 13

Sergey Bolotin
Degenerate billiards 14

Alexey Bolsinov
Stability analysis, singularities and topology of integrable systems 15

Alexey Borisov, Ivan Mamaev, Ivan Bizyaev
The Kovalevskaya top and its generalizations 16

Francisco Bulnes
Electromagnetic waves in conformal actions of the group $SU(2, 2)$ on a dimensional flat model of the space-time 17

Thierry Combot
Planar homogeneous potentials and Lotka Voltera systems 18

Vladimir Dragović, Borislav Gajić
Four-dimensional generalization of the Grioli precession 19

Holger Dullin
Twisting somersault and geometric phase 20

Nadezhda Erdakova, Ivan Mamaev
On the dynamics of a tripod sliding on a smooth surface 21

Yuri Fedorov
A shortcut to the Kovalevskaya curves 23

Bozidar Jovanovic
Modified LR and L+R systems and rolling spheres 24

Alexander Ivanov
On the control of the displacement of M-block 25

Yuri Karavaev, Alexander Kilin
Retrograde turn of rolling disk 26

Leila Khadzhieva, Vyacheslav Kruglov
Smale-Williams attractor in a modified Neimark model 27

Alexander Kilin, Evgenii Vetchanin
Controllable two-dimensional motion of a rigid body in an ideal fluid 29

Alexander Kilin, Anton Klekovkin, Elena Pivovarova
Analysis of the influence of the rolling friction on the dynamics of a robot-wheel 31

Oleg Kirillov, Mark Levi
Precession on a rotating saddle: a gyro force in an inertial frame 32

Anton Klekovkin, Ivan Mamaev
Model development of a screwless underwater robot 33

Anatoly Klenov, Evgenii Vetchanin
Theoretical and experimental investigation of the motion of a screwless overwater mobile platform 35

Nikolay Kudryashov, Dmitry Sinelshchikov
Integrability of the Liénard-type equations and non-local transformations 36

Pavel Kuptsov
Modern Lyapunov analysis: Covariant Lyapunov vectors and structure of invariant manifolds of chaotic attractors 38

Sergey Kuznetsov, Alexey Borisov, Ivan Mamaev, Valentin Tenenev
Reconstruction of model equations to the problem of the body of elliptic cross-section falling in a viscous fluid 39

Lev Lerman, Alexey Kazakov, N. Kulagin
Slow-fast dynamics of a Duffing type equation: a case of study 41

Lev Lokutsievskiy
On nilpotent approximations of non-smooth Hamiltonian systems 42

Andrzej Maciejewski, Maria Przybylska
Dynamics of chains in external fields 43

Andrzej Maciejewski, Maria Przybylska, Wojciech Szumi
Integrability obstructions of certain homogeneous Hamiltonian systems in 2D curved spaces 44

Anatoly Markeev
On the stability of two-link trajectory of the parabolic Birkhoff billiards 46

Alexey Mashtakov, R. Duits, Yu. Sachkov, E. Bekkers, I. Beschastnyi
Tracking of lines in spherical images via sub-Riemannian geodesics on SO(3) 47

Luis García Naranjo, Juan C. Marrero, Ernesto Pérez-Chavela, Miguel Rodríguez-Olmos
Relative equilibria for the 2-body problem in the hyperbolic plane 48

Luis García Naranjo, Alejandro Bravo-Doddoli
The dynamics of an articulated n-trailer vehicle 49

Grigory Osipov, V. Kostin
Transient and periodic spatiotemporal structures in reaction-diffusion-mechanics system 50

Milena Radnovic
Elliptical billiards with Hooke's potential 51

Yuri Sachkov, Yasir Awais Butt
Optimal synthesis for the left-invariant sub-Riemannian problem on the group of
hyperbolic motions of the plane 52

Igor Sataev, Alexey Kazakov
Routes to chaos in the nonholonomic model of Chaplygin top 53

Mikhail Sevryuk
Whitney smooth families of invariant tori in the reversible context 2 of KAM theory 55

Andrei Shafarevich
Classical Hamiltonian systems, Lagrangian manifolds and Maslov indices, corresponding
to spectra of Schroedinger operators with delta-potentials 57

Sergey Sokolov, Sergey Ramodanov, Pavel Ryabov
Bifurcation analysis of a 2D rigid circular cylinder interacting dynamically with a point
vortex in the absence of circulation 58

Mikhail Sokolovskiy
Nontrivial analogy of finite-core and point vortices in a two-layer rotating fluid 59

Mikhail Svinin, Yang Bai, Motoji Yamamoto
Motion planning and tracking control for a spherical rolling robot
actuated by pendulum 61

Valentin Tenenev, Evgenii Vetchanin, Lenar Ilaletdinov
Chaotic dynamics in the problem of free fall of a three-bladed screw in a fluid 62

Andrey Tsyganov
Abel equations and Backlund transformations 64

Evgenii Vetchanin, Alexey Kazakov
Dynamics of two point vortices in an external flow 65

Vasiliy Zaitsev
Uniform global asymptotic stabilization of nonlinear periodic systems by damping control 67